

Impact of Variation in Environmental Conditions on the Thermal Performance of Dry Storage Casks

Draft Report for Comment

Office of Nuclear Material Safety and Safeguards

Office of Nuclear Regulatory Research

AVAILABILITY OF REFERENCE MATERIALS IN NRC PUBLICATIONS

NRC Reference Material

As of November 1999, you may electronically access NUREG-series publications and other NRC records at NRC's Public Electronic Reading Room at <http://www.nrc.gov/reading-rm.html>. Publicly released records include, to name a few, NUREG-series publications; *Federal Register* notices; applicant, licensee, and vendor documents and correspondence; NRC correspondence and internal memoranda; bulletins and information notices; inspection and investigative reports; licensee event reports; and Commission papers and their attachments.

NRC publications in the NUREG series, NRC regulations, and Title 10, "Energy," in the *Code of Federal Regulations* may also be purchased from one of these two sources.

1. The Superintendent of Documents
U.S. Government Printing Office
Mail Stop SSOP
Washington, DC 20402-0001
Internet: bookstore.gpo.gov
Telephone: 202-512-1800
Fax: 202-512-2250
2. The National Technical Information Service
Springfield, VA 22161-0002
www.ntis.gov
1-800-553-6847 or, locally, 703-605-6000

A single copy of each NRC draft report for comment is available free, to the extent of supply, upon written request as follows:

Address: U.S. Nuclear Regulatory Commission
Office of Administration
Publications Branch
Washington, DC 20555-0001

E-mail: DISTRIBUTION.RESOURCE@NRC.GOV
Facsimile: 301-415-2289

Some publications in the NUREG series that are posted at NRC's Web site address <http://www.nrc.gov/reading-rm/doc-collections/nuregs> are updated periodically and may differ from the last printed version. Although references to material found on a Web site bear the date the material was accessed, the material available on the date cited may subsequently be removed from the site.

Non-NRC Reference Material

Documents available from public and special technical libraries include all open literature items, such as books, journal articles, transactions, *Federal Register* notices, Federal and State legislation, and congressional reports. Such documents as theses, dissertations, foreign reports and translations, and non-NRC conference proceedings may be purchased from their sponsoring organization.

Copies of industry codes and standards used in a substantive manner in the NRC regulatory process are maintained at—

The NRC Technical Library
Two White Flint North
11545 Rockville Pike
Rockville, MD 20852-2738

These standards are available in the library for reference use by the public. Codes and standards are usually copyrighted and may be purchased from the originating organization or, if they are American National Standards, from—

American National Standards Institute
11 West 42nd Street
New York, NY 10036-8002
www.ansi.org
212-642-4900

Legally binding regulatory requirements are stated only in laws; NRC regulations; licenses, including technical specifications; or orders, not in NUREG-series publications. The views expressed in contractor-prepared publications in this series are not necessarily those of the NRC.

The NUREG series comprises (1) technical and administrative reports and books prepared by the staff (NUREG-XXXX) or agency contractors (NUREG/CR-XXXX), (2) proceedings of conferences (NUREG/CP-XXXX), (3) reports resulting from international agreements (NUREG/IA-XXXX), (4) brochures (NUREG/BR-XXXX), and (5) compilations of legal decisions and orders of the Commission and Atomic and Safety Licensing Boards and of Directors' decisions under Section 2.206 of NRC's regulations (NUREG-0750).

DISCLAIMER: This report was prepared as an account of work sponsored by an agency of the U.S. Government. Neither the U.S. Government nor any agency thereof, nor any employee, makes any warranty, expressed or implied, or assumes any legal liability or responsibility for any third party's use, or the results of such use, of any information, apparatus, product, or process disclosed in this publication, or represents that its use by such third party would not infringe privately owned rights.

Impact of Variation in Environmental Conditions on the Thermal Performance of Dry Storage Casks

Draft Report for Comment

Manuscript Completed: December 2014
Date Published: February 2015

Prepared by:
Jorge Solis and Ghani Zigh

Office of Nuclear Material Safety and Safeguards

Office of Nuclear Regulatory Research

COMMENTS ON DRAFT REPORT

Any interested party may submit comments on this report for consideration by the NRC staff. Comments may be accompanied by additional relevant information or supporting data. Please specify the report number **NUREG-2174** in your comments, and send them by the end of the comment period specified in the *Federal Register* notice announcing the availability of this report.

Addresses: You may submit comments by any one of the following methods. Please include Docket ID **NRC-2014-0273** in the subject line of your comments. Comments submitted in writing or in electronic form will be posted on the NRC website and on the Federal rulemaking website <http://www.regulations.gov>.

Federal Rulemaking Website: Go to <http://www.regulations.gov> and search for documents filed under Docket ID **NRC-2014-0273**. Address questions about NRC dockets to Carol Gallagher at 301-415-3463 or by e-mail at Carol.Gallagher@nrc.gov.

Mail comments to: Cindy Bladey, Chief, Rules, Announcements, and Directives Branch (RADB), Division of Administrative Services, Office of Administration, Mail Stop: OWFN-12-H08, U.S. Nuclear Regulatory Commission, Washington, DC 20555-0001.

For any questions about the material in this report, please contact: Jorge Solis, Senior Thermal Engineer, 301-287-9094 or by e-mail at Jorge.Solis@nrc.gov.

Please be aware that any comments that you submit to the NRC will be considered a public record and entered into the Agencywide Documents Access and Management System (ADAMS). Do not provide information you would not want to be publicly available.

ABSTRACT

During the certification review of the underground long-term spent fuel dry storage cask design, the Office of Nuclear Material Safety and Safeguards (NMSS) and the Office of Nuclear Regulatory Research of the U.S. Nuclear Regulatory Commission (NRC), identified low-speed wind as an environmental factor that may affect the thermal performance of this type of design. This led NMSS to investigate the impact of wind and other environmental variables on the thermal performance of different spent fuel dry storage cask designs.

During normal conditions of storage, environmental variables, such as ambient temperature, solar heating, relative humidity, elevation, and wind speed and direction, may affect the thermal performance of a ventilated dry storage cask. The thermal evaluation of a dry storage cask generally assumes a set of fixed environmental factors (e.g., average annual ambient temperature, quiescent conditions, sea level) that will bound all sites in the continental United States. However, for some sites, using average values may not be adequate, because more adverse ambient conditions could exist for prolonged periods of time, allowing a storage system to reach new steady-state conditions that could result in higher spent fuel cladding temperatures as compared to the steady-state conditions analyzed in the cask's safety analysis report (SAR) for normal conditions of storage. For cases with predicted small thermal margin, these adverse ambient conditions could result in peak cladding temperatures exceeding recommended limits for normal conditions of storage.

This report evaluates the thermal impact of varying environmental conditions on spent fuel dry storage casks. In addition, the report investigated the transient thermal behavior of a dry storage cask when it is subjected to a sudden boundary condition change, starting from the bounding conditions described in the SAR.

The results showed that, for the underground cask design, the peak temperature in the fuel package region, represented by a homogenous composite of the gas region, the fuel, and the cladding (hereafter referred to as the peak cladding temperature (PCT)) increases for low-speed wind, as compared to quiescent conditions. The analysis also showed that the PCT starts to decrease at higher wind speeds. For vertical aboveground casks with four vents, the PCT decreased as wind speed increased. For a postulated two-air-vent vertical dry storage cask, when wind direction is normal to the air vents, the PCT decreased as the wind speed increased. When wind direction is parallel to the air vents of the two-air-vent cask, the PCT increased as the wind speed increased. For horizontal aboveground casks with air vents located on the side, the wind speed and direction did not have any significant effect on the thermal performance of the cask, as the vents are not located normal to wind. For horizontal aboveground casks with inlet vents located on the front, when wind direction is facing the front of the cask, the thermal performance of the cask was improved, but when wind direction was parallel to the cask front, no significant effect was observed.

The NRC staff should consider the analysis results in this report when performing technical reviews, applicants should consider them when applying for cask certification, and the technical reviewer should consider them for applicability to a specific design. The results can also be used as additional guidance when considering the thermal impact of the environmental factors in the thermal performance of spent fuel dry storage systems.

CONTENTS

ABSTRACT.....	iii
FIGURES.....	vii
TABLES.....	ix
ACRONYMS AND ABBREVIATIONS	xi
1.0 INTRODUCTION.....	1
1.1 Scope.....	1
1.2 Structure.....	2
2.0 ENVIRONMENTAL VARIABLES.....	3
2.1 Introduction.....	3
2.2 Ambient Temperature	3
2.3 Humidity	3
2.4 Elevation.....	3
2.5 Wind.....	4
2.6 Measured Factors.....	4
3.0 GEOMETRY AND METHOD OF ANALYSIS.....	5
3.1 Vertical Aboveground Designs.....	5
3.2 Vertical Underground Designs	5
3.3 Horizontal Aboveground Designs	5
3.4 Method of Analysis	6
4.0 ANALYZED CASES	7
4.1 Introduction.....	7
4.2 General Description of the Analyzed Casks.....	7
4.3 Three-Dimensional Cases	9
4.4 Axisymmetric Model.....	22
4.5 Flow Resistance	24
4.6 Material Properties	24
4.7 Analyzed Cases and Applied Boundary Conditions	25
4.7.1 Analyzed Three-Dimensional Cases	25
4.7.2 Applied Boundary Conditions for Three-Dimensional Analyses	25
4.7.3 Analyzed Axisymmetric Cases	26
4.7.4 Applied Boundary Conditions for the Axisymmetric Model.....	26
4.8 Discussion of Results	32
4.8.1 Wind Effect on the Underground Casks	33
4.8.2 Wind Effect on the Vertical Aboveground Casks	33
4.8.3 Wind Effect on the Horizontal Aboveground Casks	34
4.8.4 Aboveground Vertical Cask Axisymmetric Model	35
5.0 CONCLUSIONS.....	43
6.0 REFERENCES	45
APPENDIX A: EFFECTIVE THERMAL CONDUCTIVITY.....	A-1
APPENDIX B: FLOW RESISTANCE.....	B-1

FIGURES

4-1	Homogenization of the storage cell cross-section	11
4-2	Geometry and boundary conditions for HI-STORM 100 cask with four vents	12
4-3	Aboveground vertical cask with two vents (wind perpendicular to vents).....	13
4-4	Aboveground vertical cask with two vents (wind parallel to vents).....	14
4-5	Geometry and boundary conditions for the HI-STORM 100U cask.....	16
4-6	Geometry of the standardized NUHOMS cask	18
4-7	Standardized NUHOMS cask boundary conditions	19
4-8	Advanced NUHOMS cask with frontal and backward wind.....	20
4-9	Advanced NUHOMS cask with side wind	21
4-10	Homogenization of the MPC cross-section into an equivalent two-zone axisymmetric model	22
4-11	HI-STORM 100 axisymmetric model	23
4-12	Mesh generated for the air annular gap of the axisymmetric model.....	29

TABLES

2-1	Range of Environmental Variables	4
4-1	Three-Dimensional Cases Used To Study the Wind Effect	7
4-2	Axisymmetric Cases Used To Study Environmental Parameters	7
4-3	Decay Heat Values for Analyzed Casks	10
4-4	Thermo-Physical Properties of Materials Used in the Analyses.....	25
4-5	Mass Fraction Specified at Inlet Vent for Humidity Analyses.....	32
4-6	Effect of Wind Speed on Predicted PCT for HI-STORM 100U Cask.....	36
4-7	Effect of Wind Speed on Predicted PCT for HI-STORM 100 Cask with Four Vents	36
4-8	Effect of Wind Speed on Predicted PCT for HI-STORM 100 Cask with Two Vents (Wind Perpendicular to Air Vents)	36
4-9	Effect of Wind Speed on Predicted PCT for HI-STORM 100 Cask with Two Vents (Wind Parallel to Air Vents)	36
4-10	Effect of Wind Speed on Predicted PCT for Standardized NUHOMS Cask (Frontal Wind Direction)	37
4-11	Effect of Wind Speed on Predicted PCT for Standardized NUHOMS Cask (Side Wind Direction)	37
4-12	Effect of Wind Speed on Predicted PCT for Advanced NUHOMS Cask (Frontal Wind Direction)	37
4-13	Effect of Wind Speed on Predicted PCT for Advanced NUHOMS Cask (Back Wind Direction).....	37
4-14	Effect of Wind Speed on Predicted PCT for Advanced NUHOMS Cask (Side Wind Direction)	37
4-15	Transient PCT for Advanced NUHOMS Cask During Worst-Case Scenario (Back Wind Direction).....	38
4-16	Advanced NUHOMS Worst-Case Transient Scenario	38
4-17	Aboveground Vertical Cask with Two Vents—Transient Scenario.....	39
4-18	Aboveground Vertical Cask with Two Vents—Worst-Case Transient Scenario	39
4-19	Effect of Ambient Temperature on Predicted PCT (Steady-State Analysis).....	40
4-20	Transient PCT for the Effect of Ambient Temperature.....	40
4-21	Effect of Ambient Temperature on Predicted PCT (Transient Analysis)	40
4-22	Effect of Elevation on Predicted PCT (Steady-State Analysis)	40
4-23	Effect of Total Decay Heat on Predicted PCT (Steady-State Analysis).....	41
4-24	Effect of Humidity on Predicted PCT at Ambient Temperature of 300 K (Steady-State Analysis).....	41
4-25	Effect of Humidity on Predicted PCT at Ambient Temperature of 323 K (Steady-State Analysis).....	41
A-1	Spent Fuel Radial and Axial K_{eff} for the 3-D Model of the Aboveground Vertical Cask	A-1
A-2	Spent Fuel Radial and Axial K_{eff} for the 3-D Model of the Underground Vertical Cask	A-1
A-3	Spent Fuel Radial and Axial K_{eff} for the 3-D Model of the Horizontal Cask.....	A-2
A-4	Spent Fuel Axial and Radial K_{eff} for the Axisymmetric Model.....	A-2
B-1	Frictional Porous Media Flow Resistance Factors Used in ANSYS FLUENT	B-3

ACRONYMS AND ABBREVIATIONS

ASHRAE	American Society of Heating, Refrigerating and Air-Conditioning Engineers
ASME	American Society of Mechanical Engineers
BWR	boiling-water reactor
CEC	cavity enclosure container
CFD	computational fluid dynamics
CFR	<i>Code of Federal Regulations</i>
CPU	central processing unit
DO	discrete ordinates
DSC	dry-shielded canister
F	Fahrenheit
ft	feet
ISFSI	independent spent fuel storage installation
GTCC	greater than Class C
HSM	horizontal storage module
K	kelvin
kg	kilogram
km	kilometers
kW	kilowatt
m	meters
MPC	multi-purpose canister
NOAA	National Oceanic and Atmospheric Administration
NRC	U.S. Nuclear Regulatory Commission
NUHOMS	Nuclear Horizontal Modular Storage
PCT	peak cladding temperature
PWR	pressurized-water reactor
s	second
SAR	safety analysis report
SNF	spent nuclear fuel
SRP	Standard Review Plan
VVM	vertical-ventilated module
2-D	two-dimensional
3-D	three-dimensional

1.0 INTRODUCTION

The U.S. Nuclear Regulatory Commission (NRC) certifies spent fuel dry storage systems according to Title 10 of the *Code of Federal Regulations* (10 CFR) Part 72, "Licensing Requirements for the Independent Storage of Spent Nuclear Fuel, High-Level Radioactive Waste, and Reactor-Related Greater Than Class C (GTCC) Waste." The review guidance documented in "Standard Review Plan [SRP] for Spent Fuel Dry Storage Systems at a General License Facility," issued July 2010, requires a thermal evaluation for the spent fuel dry storage system to confirm that the spent fuel cladding temperatures will be maintained below recommended limits throughout the storage period, to protect the cladding against degradation that could lead to gross rupture. The thermal evaluation should identify the boundary conditions for normal, loading, off-normal, and accident conditions. The required boundary conditions include the external conditions on the cask. External ambient conditions that have a major effect on the cask's thermal performance include ambient temperature, solar heating, relative humidity, elevation, and wind speed and direction.

The cask's thermal evaluation generally assumes a set of fixed environmental factors (e.g., average annual ambient temperature, quiescent conditions, sea level) that will bound all sites in the continental United States. However, for some sites, using average values may not be adequate, because more adverse ambient conditions could exist for prolonged periods of time (for example, more than a month, as reported by the National Oceanic and Atmospheric Administration (NOAA) (NOAA Web site, www.noaa.gov) and the American Society of Heating, Refrigerating and Air-Conditioning Engineers (ASHRAE) (ASHRAE, 1997)), allowing a storage system to reach new steady-state conditions that could result in higher spent fuel cladding temperatures as compared to the steady-state conditions analyzed in the applicant's safety analysis report (SAR) for normal conditions of storage. For cases with small thermal margin, these adverse ambient conditions could result in peak cladding temperatures (PCTs) being higher than the SRP-recommended limits, which could create thermal conditions such that spent fuel could degrade and lead to gross rupture. The 10 CFR Part 72 licensing requirements mandate that storage systems be designed to allow ready retrieval of spent fuel, high-level radioactive waste, and reactor-related GTCC waste for further processing or disposal. Therefore, to comply with the applicable regulations for safe storage of spent nuclear fuel, the thermal design of a dry storage cask should demonstrate that temperatures are kept below recommended limits by considering all factors that may have an impact on the cask's thermal performance.

1.1 Scope

This document evaluates the thermal impact of varying environmental conditions on spent fuel dry storage casks. The primary goal is to examine the natural variation of the major environmental factors (ambient temperature, wind conditions, and elevation, among others) that could lead to higher spent fuel cladding temperatures as compared to the bounding thermal evaluation provided in SARs. The evaluation includes different designs to determine how the parameters considered in the evaluation affect the thermal performance of a specific design. The majority of dry storage casks that have been certified or are currently under review by the NRC include vertical and horizontal casks located aboveground and vertical underground casks (located mostly underground, except for the cask lid). Therefore, to include most of the certified designs, the study considered three casks: vertical aboveground, horizontal aboveground, and vertical underground.

1.2 Structure

This document begins with a definition of the various environmental factors that affect the cask's thermal performance and how these factors have been traditionally applied to perform the thermal evaluation of spent fuel dry storage systems. The report includes several references on the variation of these factors and how this variation affects the thermal performance of the storage systems.

This is followed by a description of the storage systems considered in the evaluation and the method of analysis used to perform the evaluation. Next, the analyzed cases are discussed, along with the results. The study concludes with recommendations on how to consider these environmental factors in the evaluation.

2.0 ENVIRONMENTAL VARIABLES

2.1 Introduction

Among the environmental variables that have a major effect on the thermal performance of a spent fuel storage system are ambient temperature, humidity, elevation, and wind magnitude and direction. Solar heating also has some effect and should be considered in the analysis. However, solar insolation values are well established and typical values are applied. NUREG-1536 states that, for storage casks, the NRC staff accepts a treatment of insolation similar to that prescribed in Title 10 of the *Code of Federal Regulations* (10 CFR) Part 71, "Packaging and Transportation of Radioactive Material," for transportation casks. Since the values specified in 10 CFR Part 71 are considered bounding, solar insolation is not considered in this study, and the investigation focuses only on the other factors (i.e., ambient temperature, humidity, elevation, and wind).

2.2 Ambient Temperature

Currently, the dry storage cask thermal evaluation includes maximum and minimum ambient temperatures as defined in the SRP (NUREG-1536, 2010). The SRP states that the NRC accepts, as the maximum and minimum "normal" temperatures, the highest and lowest ambient temperatures recorded in each year, averaged over the years of record. However, this definition does not consider seasonal variations that may result in higher maximum and minimum values. In this case, a monthly averaged value may be more appropriate for the hottest months (summer season). Measured monthly temperatures at some sites (ASHRAE, 1997) show that the annual average ambient temperature of 300 Kelvin (K) [80 degree (°) Fahrenheit (F)] could be easily exceeded for about 4 months. An ambient temperature of 300 K (80°F) is typically considered in the thermal evaluation for most of the dry casks certified by the NRC. However, the measured ambient temperatures suggest that, to bound all sites, the SAR thermal evaluation should consider seasonal variations since, during the hot months, the dry cask reaches a new steady state that the SAR has not analyzed. This study considered variations in the ambient temperature in the range of 300 to 322 K (80 to 120°F), which seems to envelope the natural variation of the ambient temperature during the hot season, according to measured data.

2.3 Humidity

Traditionally, the thermal evaluation for design certification assumes dry air, which is conservative, since humidity will increase the air thermal conductivity and heat capacity. Therefore, this study considers relative humidity in the range of 0 to 90 percent for ambient temperatures of 300 and 323 K (80 and 120°F). However, high relative humidity values do not seem to persist for the prolonged periods of time necessary for the dry cask to reach a new steady state. Therefore, this study assumes that dry air will continue to be an adequate approach, a slightly conservative assumption, as demonstrated in this evaluation.

2.4 Elevation

The thermal evaluation of dry storage casks currently assumes that the cask is located at sea level. However, the location of the dry storage cask site may have an impact on the operating pressure used to calculate the air density at the inlet vents. This, in turn, will have a direct

impact on the calculated PCT. This study considers site location in the range of 0 to 1500 meters (m) (4921.5 ft)

2.5 Wind

The thermal evaluation of dry storage casks currently assumes quiescent conditions. However, when performing the technical review of an underground dry storage cask, the staff noticed that low-speed wind [2.235 m/s (5 mph)] has a negative effect on the cask's thermal performance, as compared to quiescent conditions. Therefore, low-speed wind is considered in this study in the range of 0 to 6.706 m/s (15 mph). Reported measured values by NOAA (NOAA, www.noaa.gov) show that low-speed wind could exist for the prolonged periods of time necessary for a dry storage cask to reach a new steady state. The study considers both aboveground and underground designs and, for aboveground designs, it includes vertical and horizontal orientations to determine how low wind speed affects the thermal performance of these casks.

2.6 Measured Factors

The magnitude of the environmental variables was selected using available data from NOAA and *ASHRAE Handbook Fundamentals* (ASHRAE, 1997). Table 2-1 shows the range of the environmental variables used to investigate the effect of these factors on the thermal performance of the dry storage cask. The effect of decay heat on the dry storage cask's thermal response was also investigated, using heat sources in the range of 22 to 34 kilowatts (kW) for a specific vertical cask, as described later in this report.

Table 2-1 Range of Environmental Variables

Environmental Variable	Range
Wind Speed m/s (mph)	0–6.706 (0–15)
Ambient Temperature K (°F)	300–322 (80–120)
Humidity (%) at Ambient Temperature of 300 K (80°F)	0–90
Humidity (%) at Ambient Temperature of 323 K (120°F)	0–90
Elevation m (ft)	0–1500 (0–4921.5)

3.0 GEOMETRY AND METHOD OF ANALYSIS

3.1 Vertical Aboveground Designs

In a vertical-ventilated aboveground spent fuel storage cask design, a spent fuel canister is typically stored in a concrete overpack, with the canister bottom resting on some type of base normal to the ground. Air vents are located in the bottom and top of the overpack, so air can flow freely through the gap between the canister and the overpack to cool the canister's outer surface, thus keeping the cladding temperature below Standard Review Plan (SRP)-recommended limits (NUREG-1536, 2010). Since the inlet and outlet air vents are separated by the cask's height, thermal mixing due to low-speed wind may not have an impact on the cask's thermal performance because of the physical separation of the air vents. This separation will prevent hot air coming from the outlet vents to mix with the cooler air at the bottom of the cask. Also, hot air coming out of the outlet vents will tend to flow up into the ambient air surrounding the cask. However, low-speed wind could block the air vents, which could have an impact on the cooling effect by reducing the mass flow rate through the annular gap. Therefore, this study includes this cask to determine the effect of other environmental factors and to conclusively determine how low-speed wind affects this design.

3.2 Vertical Underground Designs

In an underground design, the canister is stored inside some type of enclosure that is buried almost entirely, except for the overpack lid, which is located aboveground and includes the air vents. In this design, air needs to flow downwards into the enclosure container and then upwards in contact with the canister's outer shell. Decay heat from the spent fuel assemblies stored in the canister is thus dissipated through the canister's outer wall by a combination of convection, radiation, and conduction to flowing air. Finally, hot air exits through the outlet vent, which is located on top of the cask lid. For this design, the inlet and outlet vents are located in proximity to each other. These design features represent a challenge from the analysis point of view since, in addition to the typical environmental factors used in the thermal evaluation (e.g., ambient temperature, ambient pressure), the analysis must include other factors such as low wind speed. This increases both the complexity and the computational times, since usually three-dimensional (3-D) thermal models are needed to properly capture the heat transfer and flow characteristics of this design.

3.3 Horizontal Aboveground Designs

In a horizontal spent fuel storage cask, a spent fuel canister is typically stored in a concrete overpack with the canister side resting on some type of base, normal to the ground. Inlet vents are located on the front or side of the bottom of the overpack. Outlet vents are located on the top side of the overpack or on the roof. Decay heat from the spent fuel assemblies stored in the canister is thus dissipated through the canister's outer wall by a combination of convection, radiation, and conduction to flowing air.

The heat transfer characteristics of these designs are almost identical, except for the vertical configuration, where convection heat transfer inside the canister plays an important role, especially for pressurized canisters. Since the geometry is different for the three designs, some of the environmental variables (especially low-speed wind) will affect the thermal performance in a different manner (due to the design and location of the air vents).

3.4 Method of Analysis

The analysis used computational fluid dynamics (CFD) methods, using the ANSYS FLUENT software as the primary analytical tool. ANSYS FLUENT (Fluent, 2006) is a CFD code that solves the governing equations for the conservation of mass and momentum and (when necessary) for energy and other scalar quantities, such as turbulence and chemical species concentrations. ANSYS FLUENT uses a control-volume-based technique to convert a general scalar transport equation to an algebraic equation that is solved numerically. The following steps are used to solve the algebraic equations:

- (a) division of the domain into discrete control volumes using a computational grid
- (b) integration of the governing equations on the individual control volumes to construct algebraic equations for the discrete dependent variables (“unknowns”), such as velocities, pressure, temperature, and conserved scalars
- (c) linearization of the discretized equations and solution of the resultant linear equation system to yield updated values of the dependent variables

Two-dimensional (2-D) and 3-D thermal models can be built and a solution obtained using the ANSYS FLUENT CFD code. This study considered both 2-D axisymmetric and 3-D thermal models to study the impact of a variety of environmental conditions on the thermal performance of spent fuel dry storage casks. Wind studies used both axisymmetric and 3-D thermal models to perform both steady-state and transient analyses. For the other environmental parameters, only axisymmetric steady-state and transient analyses were applied to reduce the central processing unit (CPU) time to perform the analyses. Chapter 4 contains specific details of the developed thermal models used in this evaluation.

4.0 ANALYZED CASES

4.1 Introduction

The NRC developed two types of thermal models to study the environmental variables: a 3-D model for the wind study and a 2-D axisymmetric model to study the effect of the other parameters. Table 4-1 shows the cask systems selected to analyze the effect of wind on the dry storage cask's thermal performance. Table 4-2 shows the 2-D axisymmetric cases used to investigate the effect of humidity, ambient temperature, altitude, decay heat, and wind. In this study, the axisymmetric model is a representation of an aboveground vertical storage system.

Table 4-1 Three-Dimensional Cases Used To Study the Wind Effect

Orientation	Location	Dimensions	Mode of Analysis
Vertical (HI-STORM 100)	Aboveground	3-D	Steady
Vertical (HI-STORM 100U)	Underground	3-D	Steady
Horizontal (Standardized NUHOMS)	Aboveground	3-D	Steady
Horizontal (Advanced NUHOMS)	Aboveground	3-D	Steady & Transient

Table 4-2 Axisymmetric Cases Used To Study Environmental Parameters

Variable	Dimensions	Mode of Analysis
Ambient Temperature	2-D	Steady & Transient
Humidity	2-D	Steady
Altitude	2-D	Steady
Heat load	2-D	Steady
Wind	2-D	Transient

4.2 General Description of the Analyzed Casks

Three different spent fuel dry cask designs, HI-STORM 100, HI-STORM 100U, and NUHOMS, were selected to develop the thermal models used in this study. These casks cover the variety of designs to determine the effect of different environmental factors, especially the effect of wind. These designs also cover the different geometries of interest (i.e., vertical, horizontal, aboveground, and underground designs). The analysis results can be used to evaluate similar designs (e.g., vertical orientation, number of air vents). The environmental factors considered in this study affect all storage systems, and low-speed wind only affects ventilated storage

systems because of the presence of discrete vents, in the case of aboveground designs, or blockage of the air vents and the proximity of the inlet and outlet vents, in the case of underground designs.

HI-STORM 100

The HI-STORM 100 (Holtec Storage and Transfer Operation Reinforced Module) spent fuel cask storage system consists of a sealed canister positioned inside a vertical ventilated storage overpack (Holtec International, 2005). Four inlet and outlet ducts that allow for air cooling of the stored multipurpose canister (MPC) are located at the bottom and top, respectively, of the storage overpack. The spent nuclear fuel (SNF) assemblies are located inside the MPC, which is sealed with a welded lid to form the confinement boundary. The MPC contains an all-alloy honeycomb basket structure with square-shaped compartments of appropriate dimensions to allow insertion of the spent fuel assemblies before welding the MPC. The MPC basket designs are designated as MPC-32 (for holding up to 32 pressurized-water reactor (PWR) spent fuel assemblies), MPC-24 (for holding up to 24 PWR spent fuel assemblies) and MPC-68 (for holding up to 68 boiling-water reactor (BWR) spent fuel assemblies). After vacuum drying, the MPC is backfilled with helium to provide a stable, inert environment for long-term storage of the SNF. The helium gas fills all the space between the solid components and provides an improved conduction medium for dissipating decay heat in the MPC. During normal storage conditions in the HI-STORM 100 storage system, heat is rejected from the SNF to the environment by passive heat transfer mechanisms only.

HI-STORM 100U

The HI-STORM 100U spent fuel storage system (Holtec International, 2007) uses an underground vertical-ventilated module (VVM) designed to accept all MPC models (e.g., MPC-24, MPC-32) for storage at an independent spent fuel storage installation (ISFSI). The VVM provides for storage of MPCs in a vertical configuration inside a subterranean cylindrical cavity entirely below the top-of-the-grade of the ISFSI. The MPC storage cavity is defined by the cavity enclosure container (CEC), consisting of the container shell integrally welded to the bottom plate. The top of the container shell is stiffened by the container flange (a ring-shaped flange) that is also integrally welded. All of the constituent parts of the CEC are made of thick low-carbon steel plate. In its installed configuration, the CEC is interfaced with the surrounding subgrade for most of its height, except for the top region, where it is girdled by the top ISFSI pad. The cylindrical surface of the divider shell is equipped with insulation to ensure that the heated air streaming up around the MPC in the inner coolant air space causes minimal preheating of the air streaming down the intake plenum. After vacuum drying, the MPC is backfilled with helium to provide a stable, inert environment for long-term storage of the SNF. In the HI-STORM 100U system, heat is rejected from the SNF to the environment by passive heat transfer mechanisms only. Air intake and outlet vents are located on the cask lid. The VVM is engineered for outdoor below-grade storage for the duration of its design life, and it is designed to withstand normal, off-normal, and extreme environmental phenomena as well as accident storage conditions.

STANDARDIZED AND ADVANCED NUHOMS

The standardized and advanced horizontal storage module (HSM), the NUHOMS (Nuclear Horizontal Modular Storage) spent fuel storage system, provides for the horizontal storage of

irradiated fuel in a dry-shielded canister (DSC) that is placed in a concrete horizontal storage module (Transnuclear, Inc., 2006, 2008). Decay heat is removed from the spent fuel by conduction and radiation within the DSC and by convection and radiation from the surface of the DSC. The natural circulation flow of air through the HSM and the conduction of heat through concrete provide the mechanisms of heat removal from the HSM.

Spent fuel assemblies are loaded into the DSC while it is inside a transfer cask in the spent fuel pool at the reactor site. The transfer cask containing the loaded DSC is removed from the pool, dried, purged, backfilled with helium, and sealed. The loaded DSC inside the transfer cask is moved to the HSM, where it is pushed into the HSM by a horizontal hydraulic ram. The DSC is constructed from stainless-steel plates and contains a basket consisting of a number of square cells in either the PWR or the BWR design. An intact spent fuel assembly is loaded into each cell yielding a capacity of 24, 32, and 37 PWR or 52, 61, and 69 BWR spent fuel assemblies per DSC. Spacer disks are used for structural support. The DSC has double seal welds at each end and rests on two steel rails when placed in the HSM.

The HSM is constructed from reinforced concrete, carbon steel, and stainless steel. Passageways for air flow through the HSM are designed to minimize the escape of radiation from the HSM but also to permit adequate cooling air flow. Decay heat from the spent fuel assemblies within the canister is removed from the DSC by natural draft convection and radiation. Air enters along the bottom of each side of the HSM, flows around the canister, and exits through flow channels along the top sides of the module. Heat is also radiated from the DSC to the inner surface of the HSM walls where, again, natural convection air flow removes the heat. Some heat is also removed by conduction through the concrete.

The horizontal NUHOMS casks are designed to passively remove heat from the DSC by natural circulation of airflow through the cask. The NUHOMS casks are located on a reinforced concrete pad and fastened to adjacent HSM casks. For design-basis seismic events, a minimum of three casks must be fastened together. In the analysis, the main difference between the two types of NUHOMS horizontal casks is the placement of the vents and the airflow path inside the cask. The standardized NUHOMS cask has two inlet vents on both sides at the bottom of the cask and two outlet vents on both sides at the top. The Advanced HSM has one inlet air vent at the bottom on the front of the cask and one outlet air vent on the roof of the cask.

4.3 Three-Dimensional Cases

For long-term storage conditions, the cask's thermal evaluation follows the guidelines of NUREG-1536, with the canister cavity backfilled with helium. Thermal analysis results for the long-term storage scenarios and short-term transient conditions are obtained and presented in this report, focusing on the effect of varying environmental conditions on the thermal performance of the spent fuel dry storage cask. The boundary condition used to represent wind is located at an adequate distance to prevent any interference with the cask vents and walls. The distance of the velocity and pressure boundaries is carefully selected to obtain physically meaningful results. If these boundaries are too close to the cask boundaries (external walls, air vents), unrealistic air velocities would be developed, which would affect the analysis results (American Society of Mechanical Engineers (ASME), "Standard for Verification and Validation in Computational Fluid Dynamics and Heat Transfer," 2009).

HI-STORM 100

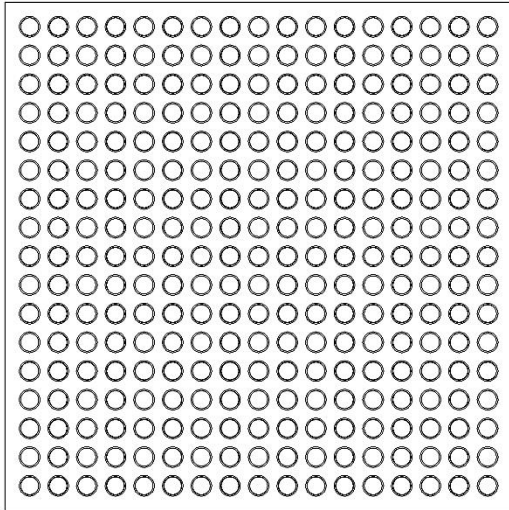
The MPC basket that holds the spent fuel assemblies is a matrix of interconnected square compartments designed to hold the spent fuel assemblies in a vertical position under long-term storage conditions. The basket is a honeycomb structure of stainless-steel plates with full-length welded intersections to form an integral basket configuration. All individual cell walls, except outer periphery cell walls, are provided with neutron absorber plates sandwiched between the box wall and a stainless-steel sheathing plate over the full length of the active spent fuel region. The neutron absorber plates used in all MPCs are made of an aluminum-based material containing boron carbide to provide criticality control while maximizing heat conduction capabilities. Heat generation in the MPC is axially nonuniform because of nonuniform axial burnup profiles in the spent fuel assemblies. Table 4-3 shows the design-basis decay heat for long-term normal storage for the analyzed casks. The decay heat is conservatively considered to be nonuniformly distributed over the active spent fuel length, based on a prescribed axial burnup distribution.

Table 4-3 Decay Heat Values for Analyzed Casks

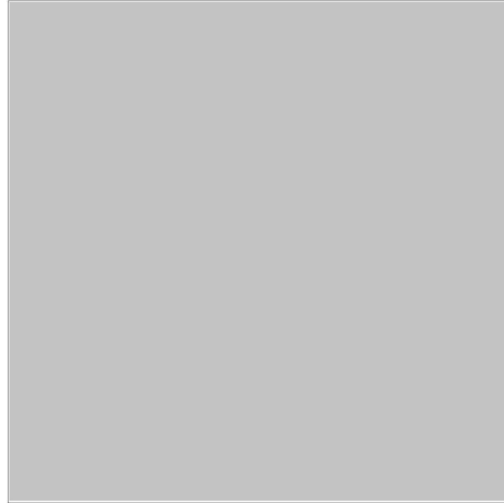
Cask Type	Decay Heat (kW)
HI-STORM 100	34
HI-STORM 100U	36.9
Standardized NUHOMS	24
Advanced NUHOMS	24

The thermal analysis used two different thermal models: a half-symmetry 3-D model and a 2-D axisymmetric model. Both models use porous media to represent the flow through the spent fuel rods. Porous media are used to represent the spent fuel assembly in the 3-D model, as shown in Figure 4-1. Flow resistance factors that characterize the spent fuel regions are obtained from separate calculations using CFD. These calculations include all important features that contribute to flow resistance (e.g., spent fuel rods, spacers, water rods). Other than representing the spent fuel assemblies using porous media, the 3-D model explicitly represents all major components (e.g., spent fuel basket, helium inside the cavity, MPC shell, air gap between the MPC shell and overpack, concrete overpack). Figures 4-2, 4-3, and 4-4 show the model graphically. The two-vent 3-D thermal model is identical to the four-vent model, except for the number of vents.

Thermal analysis results from a 3-D model were used to evaluate the effect of wind on the different cask configurations, as shown in Table 4-1. The analyses considered wind velocities varying between 0 and 6.706 m/s (0 and 15 mph). The analyses also considered bounding wind directions for wind approaching the air vents (e.g., parallel to vent, normal to vent). For the 0 m/s wind case that represents normal quiescent conditions, the pressure boundary was specified all around the dry storage cask control volume. For nonquiescent conditions (low-speed wind), inlet velocity [varying between 0 and 6.706 m/s (0 and 15 mph)] was applied on the wind side and pressure boundary on the opposite side.

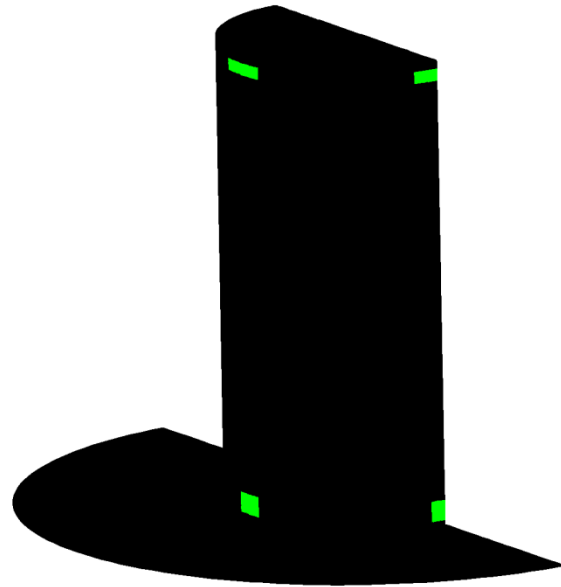
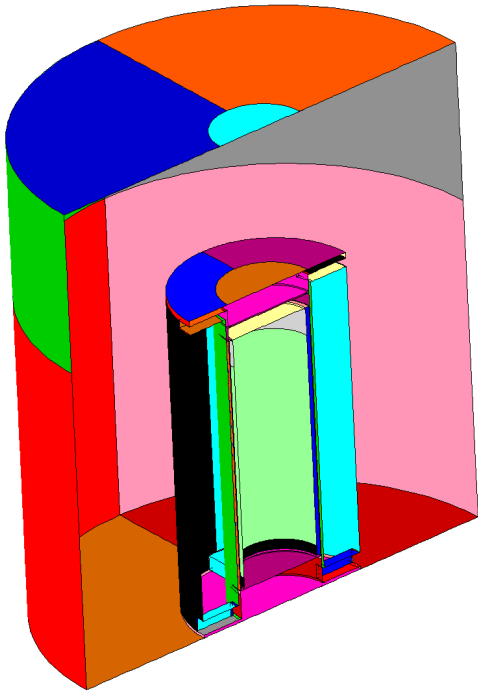


(a) Detailed spent fuel cell

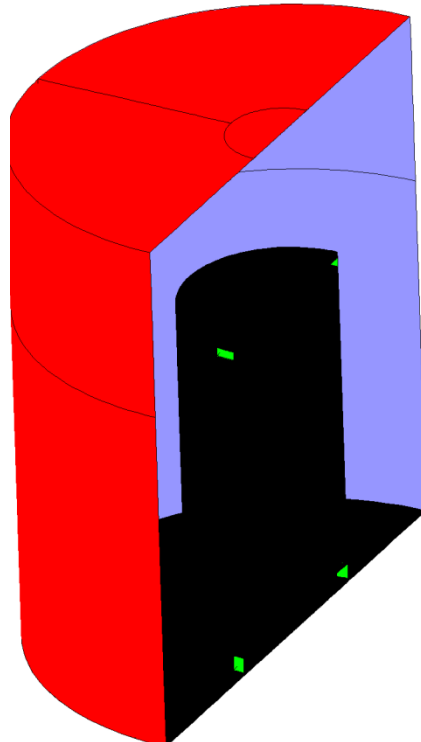
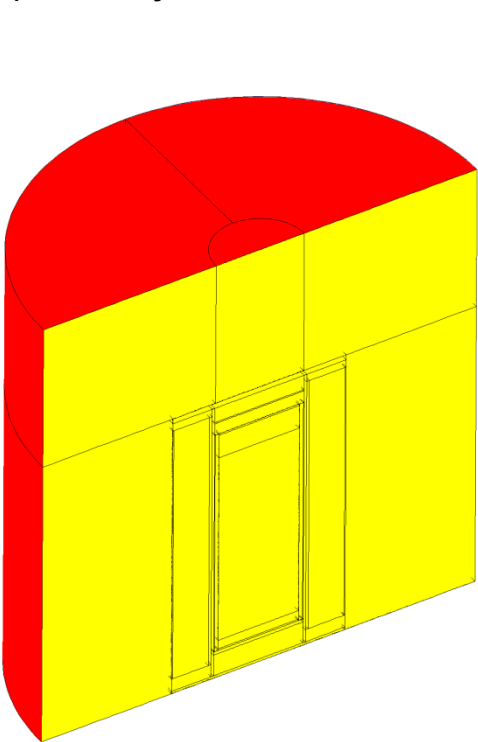


(b) Homogenized cross-section

Figure 4-1 Homogenization of the storage cell cross-section

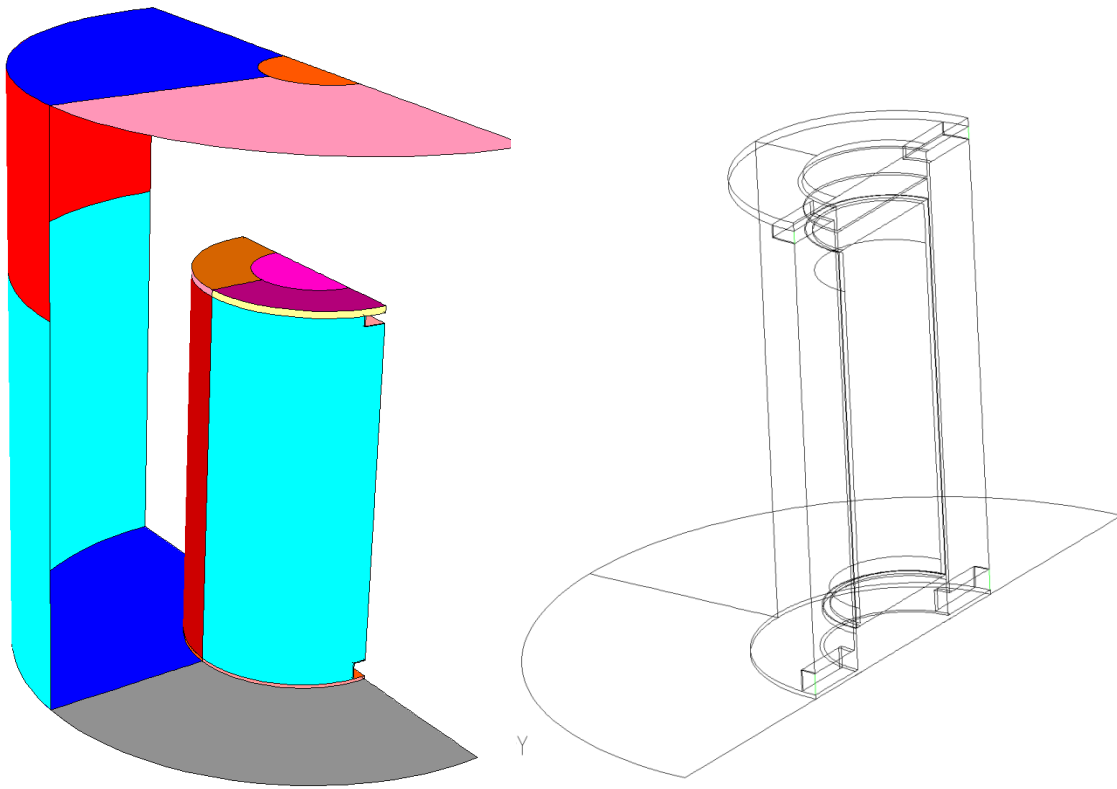


(a) Geometry

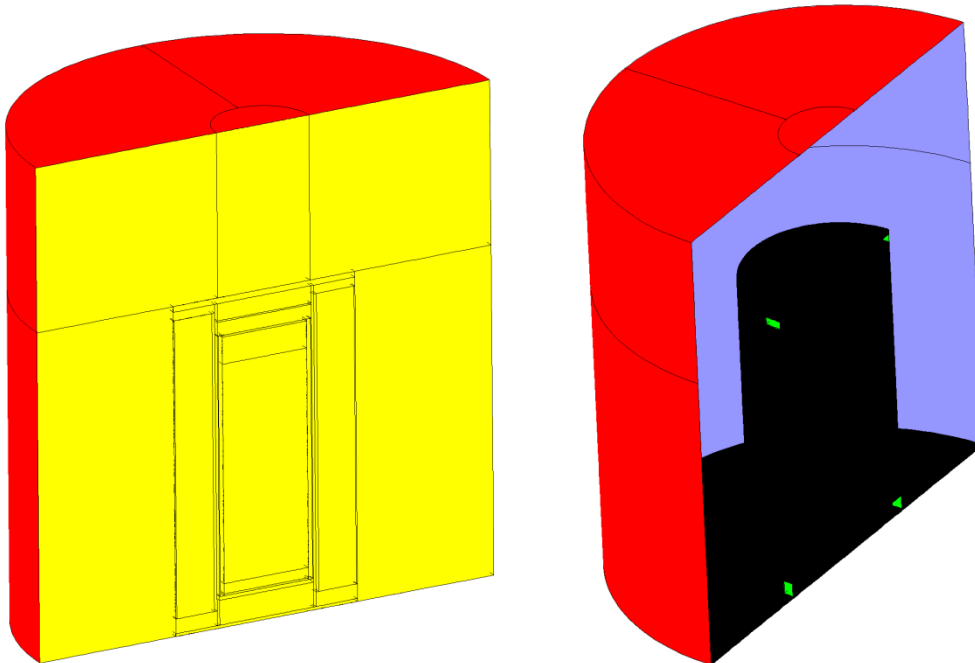


(b) Boundary Conditions

Figure 4-2 Geometry and boundary conditions for HI-STORM 100 cask with four vents

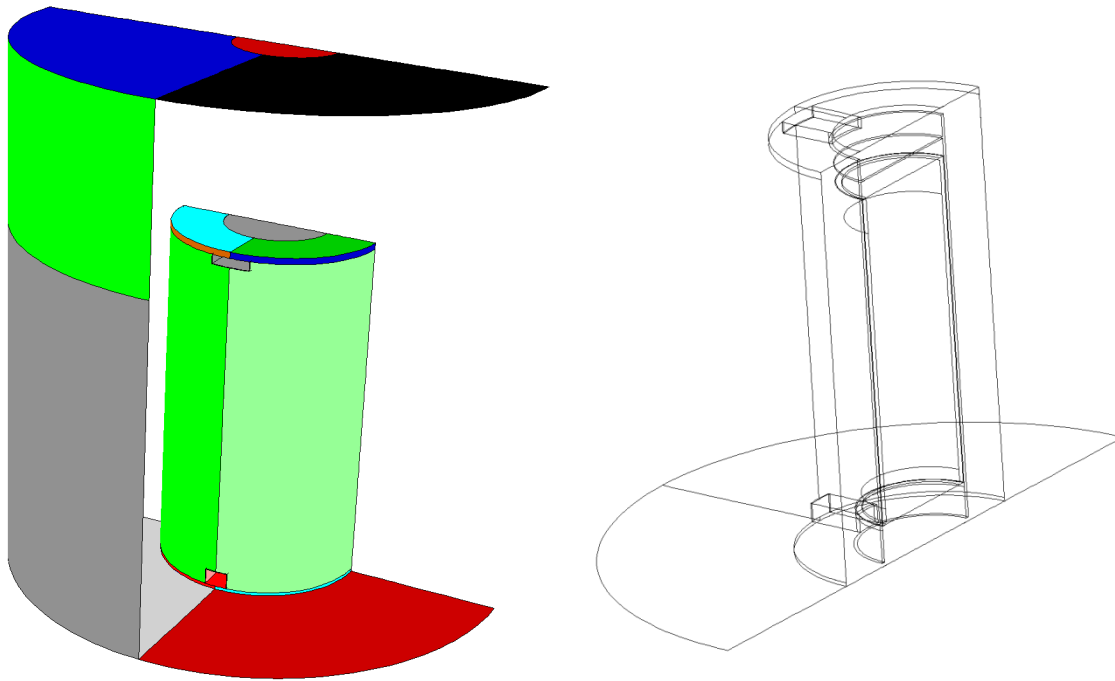


(a) Geometry

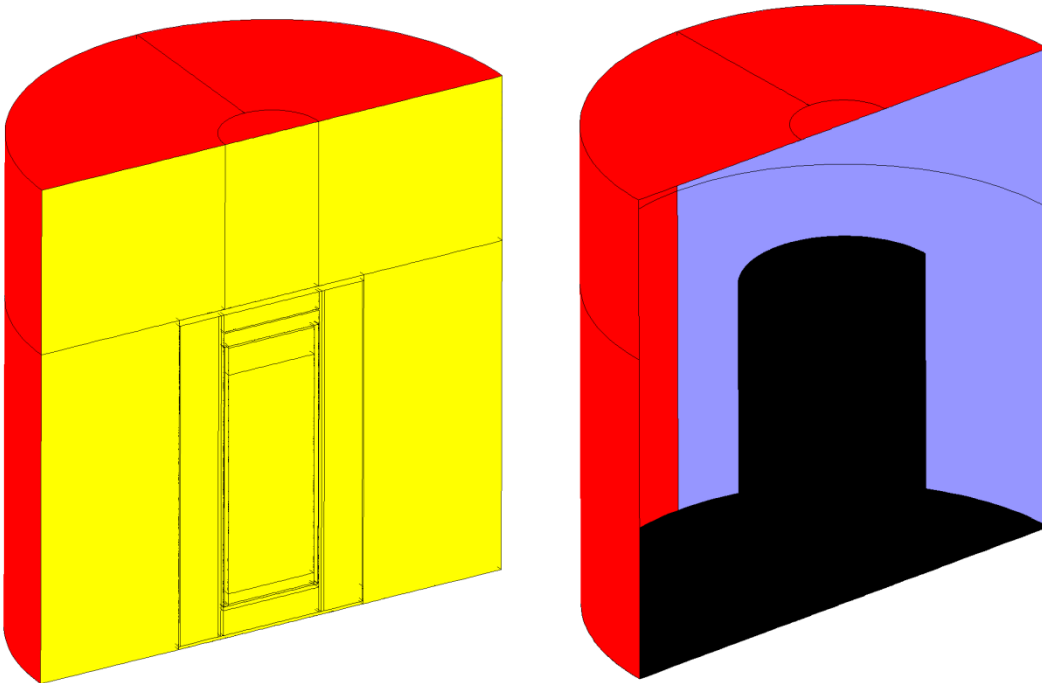


(b) Boundary conditions

Figure 4-3 Aboveground vertical cask with two vents (wind perpendicular to vents)



(a) Geometry

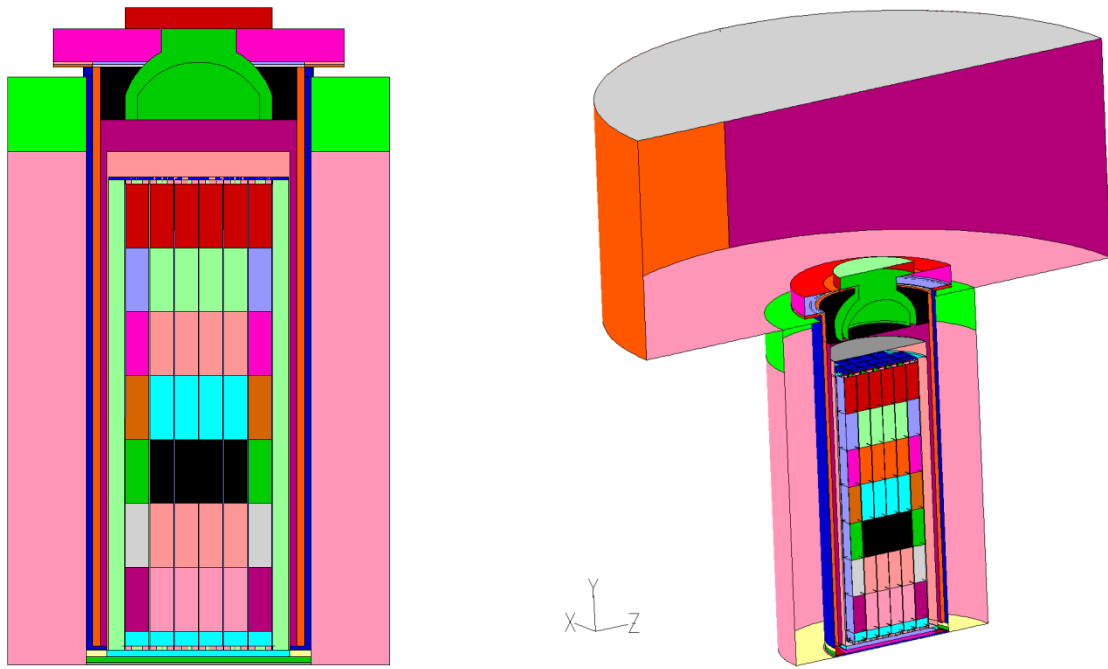


(b) Boundary conditions

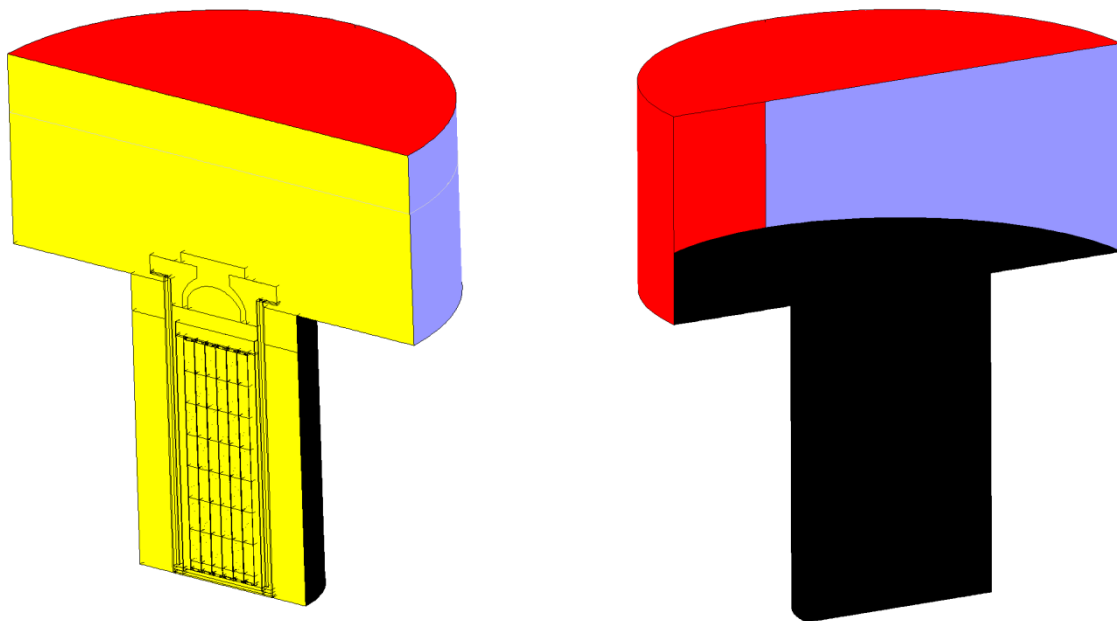
Figure 4-4 Aboveground vertical cask with two vents (wind parallel to vents)

HI-STORM 100U

A one-half symmetry 3-D thermal model was developed to perform the environmental study, as seen in Figure 4-5, which shows that, except for the spent fuel region, all major components are represented explicitly in the thermal model. As described earlier, the spent fuel assembly is represented using porous media characterized by flow resistance factors calculated separately and effective thermal conductivity, as described in Appendix A, "Effective Thermal Conductivity" (TRW report, "Spent Nuclear Fuel Effective Thermal Conductivity Report," 1996). Figure 4-5(a) shows the pictorial representation of the cask and the environment associated with it. Figure 4-5(b) shows the boundary conditions used in the model. Applied boundary conditions include symmetry, velocity inlet (to represent wind), and pressure inlet (to represent the boundary limits on the environmental side). A wall is used to represent the top of the ground and the enclosure wall of the cask cavity.



(a) Geometry



(b) Boundary conditions

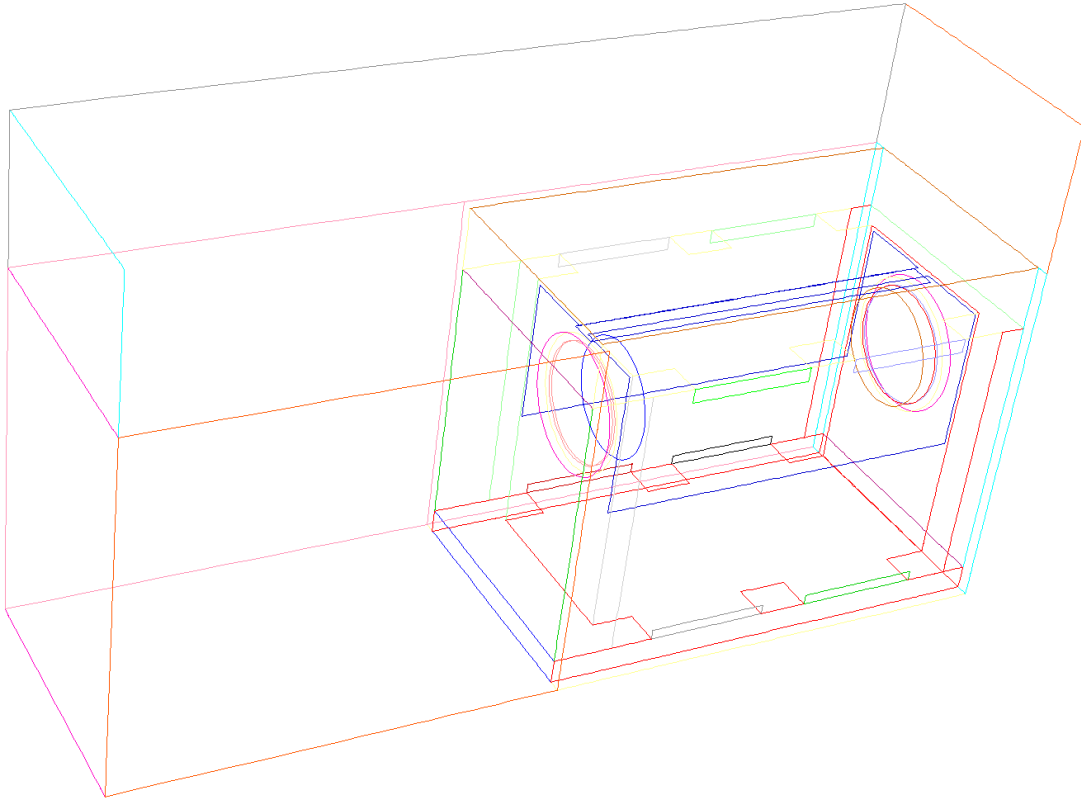
Figure 4-5 Geometry and boundary conditions for the HI-STORM 100U cask

NUHOMS

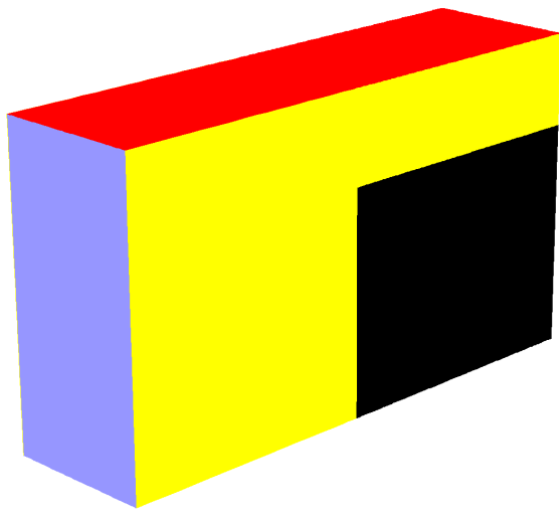
A full geometry thermal model was built to represent this system. This study considered two versions of the cask design: standardized and advanced. The location of the air vents is the main difference between these versions from the point of view of wind effect. The developed models are shown in Figures 4-6 and 4-7 for the standardized version and Figures 4-8 and 4-9 for the advanced version. The thermal models developed for the NUHOMS casks include all important features that play a role in determining the effect of wind. For example, the DSC is represented as a solid body with heat generation distribution approximated to a standard axial power profile. The model includes all internal main features of the horizontal overpack except the cask support structures, since they have a minor effect. The main objective of this study was to obtain the relative effect on the PCT and not the approximate PCT value. The thermal results from the wind study are compared to quiescent conditions.

Figure 4-6 shows the standardized NUHOMS casks' geometry as represented in the thermal model and the boundary conditions applied to the analysis. Since the model is assumed to be located in a row of casks, symmetry boundary conditions are applied to both sides of the extended model, along with the wall represented by an adjacent cask (symmetry: yellow and wall: black). The velocity inlet boundary is located at a sufficient distance to allow the development of the air flow and avoid any effect on the cask air vents (inlet velocity: blue). The top of the cask is represented as a pressure boundary (red) and the back is partly represented with an adiabatic wall to represent an adjacent cask. The part of the back of the control volume that is part of the back wall is assigned a pressure boundary to represent the environment. Figure 4-7 shows the boundary conditions applied to the standardized NUHOMS model to analyze the wind effect. Two bounding directions were considered: frontal wind and side wind (shown in blue).

The boundary conditions applied to the thermal model of the advanced NUHOMS cask are shown in Figures 8 and 9. The main difference between this design and the standardized version is the location of the air vents. In the standardized version, the vents are located on the side of the cask while, for the advanced NUHOMS cask, they are located on the front and top (towards the back). The wind study considered three cases: whether the wind was blowing towards the front, back, or side of the cask.

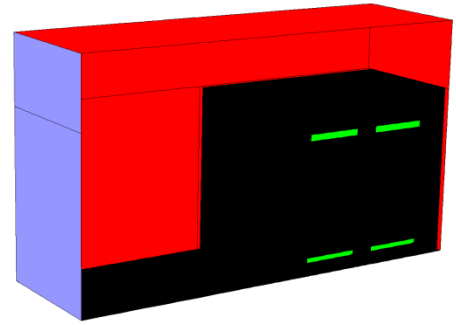
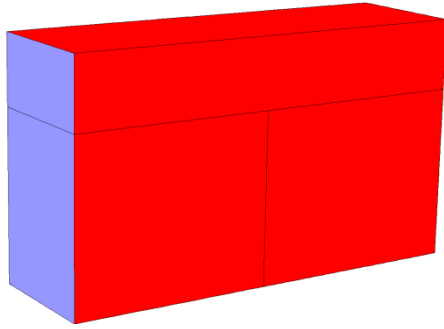


(a) Geometry

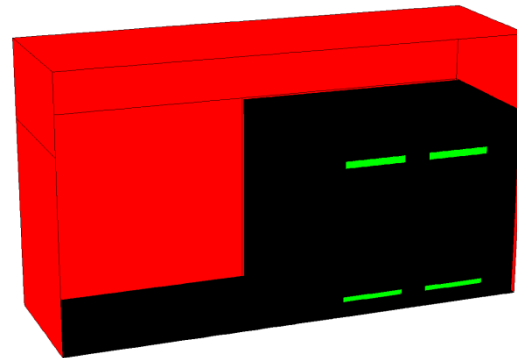
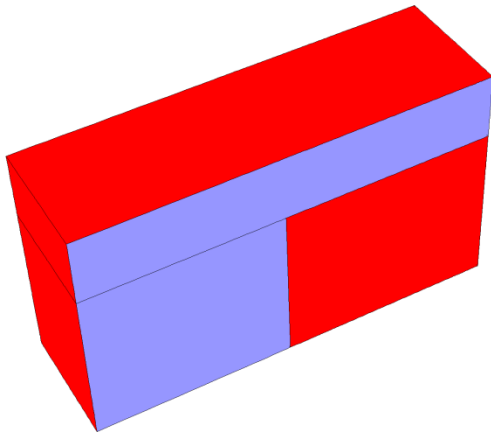


(b) Boundary Conditions

Figure 4-6 Geometry of the standardized NUHOMS cask



(a) Frontal wind



(b) Side wind

Figure 4-7 Standardized NUHOMS cask boundary conditions

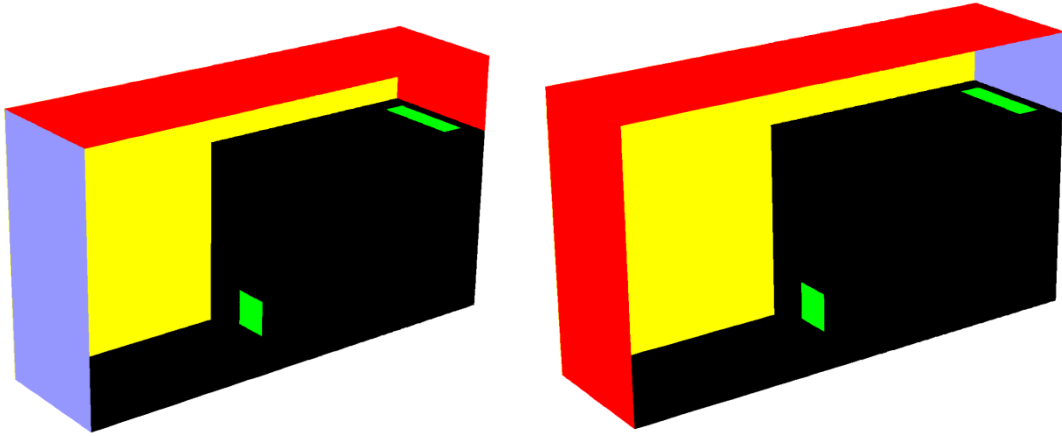
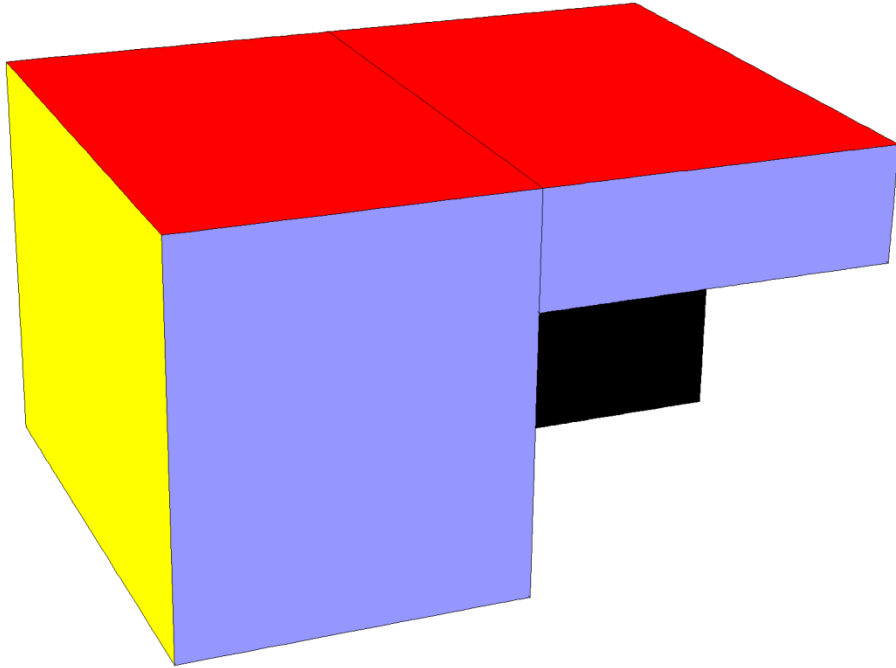
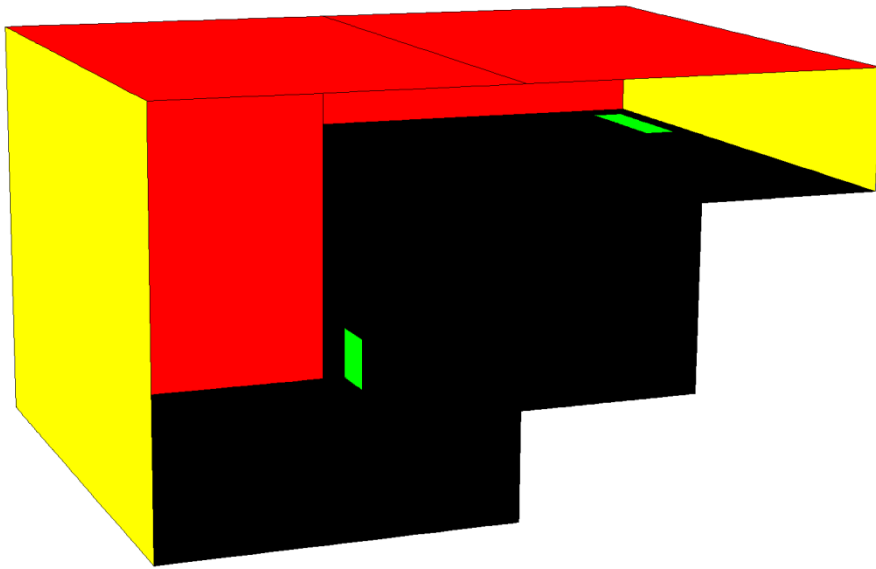


Figure 4-8 Advanced NUHOMS cask with frontal and backward wind



(a) External boundary



(b) Air vents

Figure 4-9 Advanced NUHOMS cask with side wind

4.4 Axisymmetric Model

For the HI-STORM 100 axisymmetric thermal model, the basket is homogenized into an equivalent cylindrical volume, as shown in Figure 4-10. The spent fuel basket and the spent fuel assemblies are homogenized, and the equivalent thermal properties and flow resistance factors are calculated separately and used in the axisymmetric model. Figure 4-11 shows an axial representation of the axisymmetric model with its main features (homogenized basket with axial power distribution, upper plenum, downcomer, lower plenums, MPC, air gap between the MPC shell and the concrete overpack, inlet and outlet vents, and overpack).

The axisymmetric model was used to analyze the steady-state effect of the ambient temperature, humidity, elevation, and heat load, as shown in Table 4-2. The axisymmetric model was also used to study the transient dry storage cask thermal response for the worst-case wind scenario (i.e., two-vent vertical dry storage cask with wind parallel to air vents), as well as the transient thermal behavior during a sudden change in the ambient temperature.

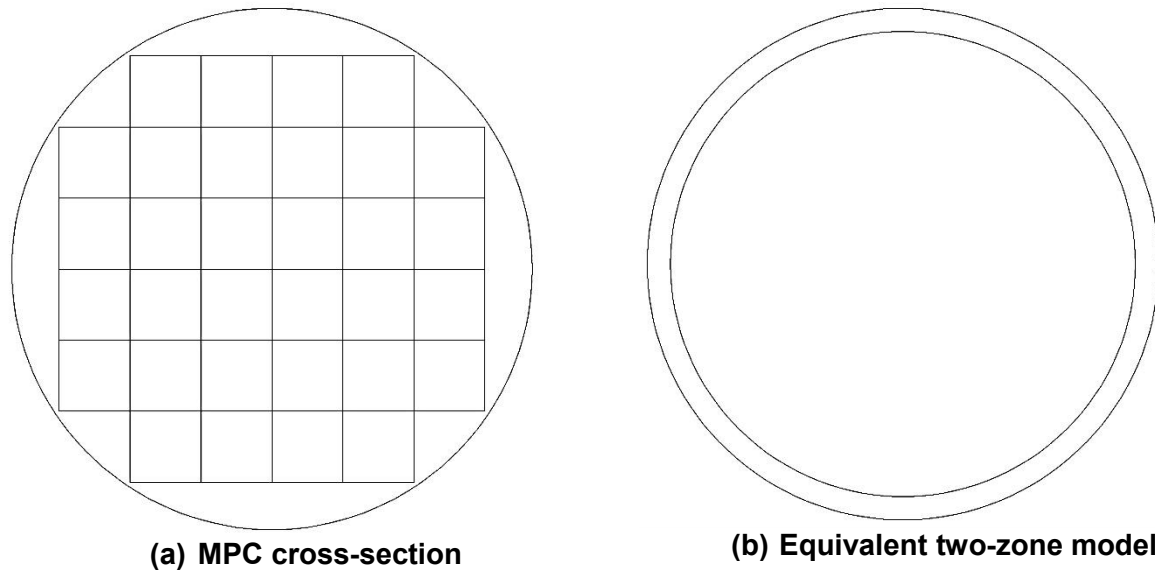


Figure 4-10 Homogenization of the MPC cross-section into an equivalent two-zone axisymmetric model

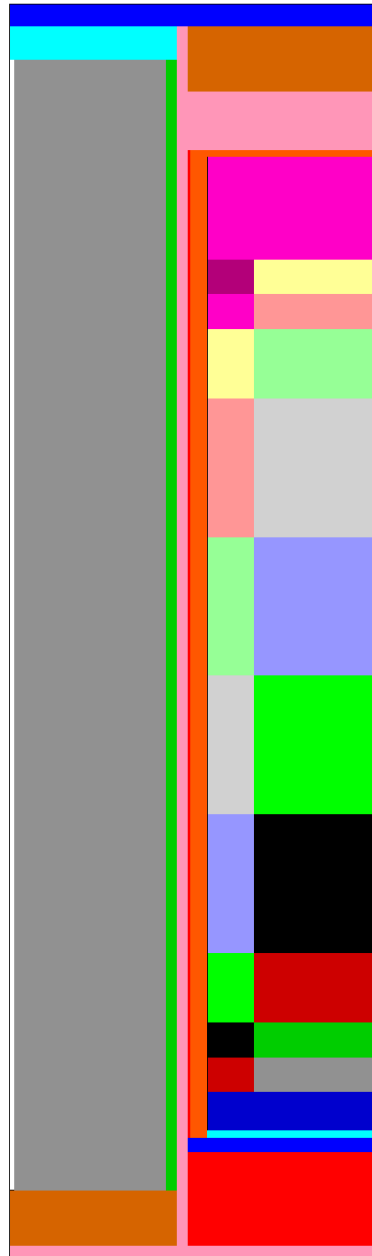
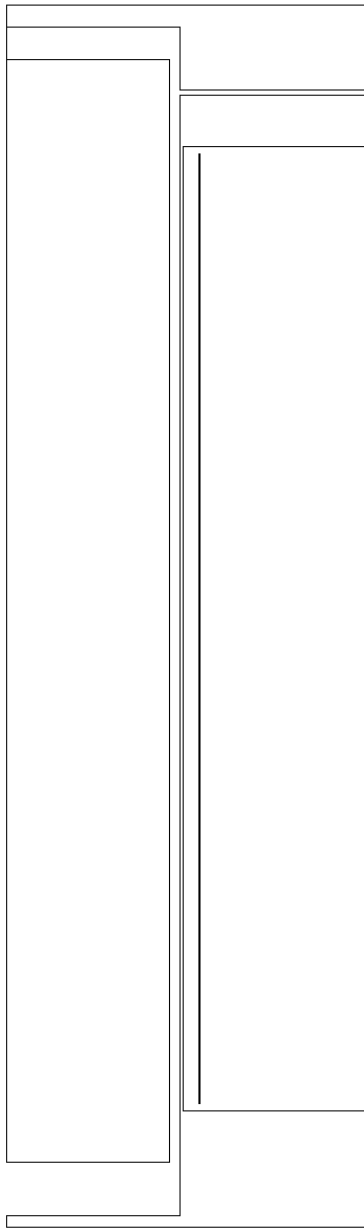


Figure 4-11 HI-STORM 100 axisymmetric model

4.5 Flow Resistance

The casks are evaluated for storing a specific arrangement of either BWR or PWR spent fuel assemblies. During spent fuel storage in the vertical configuration, helium enters the basket storage cells from the bottom plenum, flows upward through the open spaces in the spent fuel storage cells, and exits through the top plenum. The top and bottom plenums are essentially open spaces engineered in the spent fuel basket ends to enable helium circulation. In the case of BWR spent fuel storage, a channel enveloping the spent fuel bundle divides the flow into two parallel paths. One flow path is through the in-channel or rodded region of the storage cell, and the other flow path is in the square annulus outside the channel. The two modeling approaches below simulate heat transfer and fluid flow in the dry storage cask.

The first approach uses a 3-D representation of the dry storage cask. In this model, the spent fuel basket was modeled using porous media inside the spent fuel storage cells (for the PWR spent fuel assemblies) and porous media inside the spent fuel channel (for the BWR spent fuel assemblies). For the BWR spent fuel storage configuration, the square annular gap between the spent fuel channel and the basket storage cell is represented explicitly as a helium flow path. Therefore, the canister is modeled as a 3-D array of square-shaped cells (basket) inside a cylindrical canister shell.

The second approach uses an axisymmetric model to represent the entire cask. To avoid modeling the individual spent fuel rods, porous media were used to represent any volume enclosing the spent fuel rods.

In the ANSYS FLUENT CFD code, porous media viscous flow resistance is modeled as follows:

$$\Delta P = D\mu VL$$

Where ΔP is the hydraulic pressure loss, D is the flow-resistance coefficient, μ is the fluid viscosity, V is the superficial fluid velocity, and L is the porous media length. In the model, the spent fuel storage cell length between the bottom and top plenums is replaced by porous media.

To characterize the flow resistance of spent fuel assemblies inside the spent fuel basket region, a 3-D model of either PWR or BWR spent fuel assemblies is constructed using the ANSYS FLUENT CFD program (NUREG-2152, "Computational Fluid Dynamics Best Practice Guidelines for Dry Cask Applications," issued March 2013). In this model, the spent fuel rods, water rods, and grid spacers are represented explicitly. The 3-D flow-resistance model used two approaches to calculate the flow resistance. The first approach is the pressure-drop method and the second is the shear-stress method. Both methods are applied for sections without flow area changes (i.e., no contractions or expansions). Both approaches are related and should lead to the same values (Appendix B, "Flow Resistance"). Table B-1 of Appendix B shows the obtained resistance values used in both the 3-D models and the axisymmetric model.

4.6 Material Properties

Materials present in the storage canisters include stainless steel, neutron absorber (Boral or METAMIC), and helium. Materials present in the storage cask overpacks include carbon steel and concrete. Table 4-4 presents a summary of material properties used for performing all thermal analyses.

Table 4-4 Thermo-Physical Properties of Materials Used in the Analyses

Material	Emissivity	Conductivity	Heat Capacity	Density
Helium	n/a	Kinetic Theory [Robert C Reid et al., 1977]	Cp(T) [JANAF, 1985]	Ideal gas law
Air	n/a	Kinetic theory [Robert C Reid et al., 1977]	Cp(T) [JANAF, 1985]	Ideal gas law
Carbon Steel	0.85	42.2	n/a	n/a
Alloy X	0.587	K(T) [Holtec International, 2005]	n/a	n/a
Concrete	n/a	1.81	n/a	n/a
Zircaloy	0.8	K(T) [Holtec International, 2005]	n/a	n/a

4.7 Analyzed Cases and Applied Boundary Conditions

4.7.1 Analyzed Three-Dimensional Cases

The wind-effect analysis used half-symmetry models to minimize CPU time and effort to analyze the HI-STORM 100 and HI-STORM 100U dry storage casks. Due to the lack of symmetry, full symmetry models were used to analyze the NUHOMS dry storage casks for wind studies. However, to simplify the analysis, the canister was modeled as a solid cylinder with a decay heat power profile representative of the type of fuel stored in the horizontal canisters. Turbulence was modeled using the low Reynolds $k-\epsilon$ model. The discrete ordinate (DO) thermal radiation model was selected to model the radiative transfer equation. Table 4-1 shows the different 3-D cases that were considered to analyze the effect of wind on the thermal performance of different cask designs and configurations.

4.7.2 Applied Boundary Conditions for Three-Dimensional Analyses

The modeled cask will be located inside a control volume that represents the environment. Therefore, the external boundary conditions (environment surrounding the dry storage cask) were represented in the ANSYS FLUENT model by specifying appropriate inlet velocities (wind side) or pressures (wind opposite side) and ambient temperature.

As stated previously, the external boundary conditions on the modeled dry storage cask consisted of a velocity inlet on the direction of wind side, a pressure outlet on the side opposing wind direction and the top sides, and symmetry for the sides that are orthogonal to the wind direction, as shown in Figures 4-2 through 4-9. When only half of the cask was modeled, as in the HI-STORM 100U and HI-STORM 100 (with four vents and two vents), symmetry was assumed on the plane dividing the cask in half. Thermal radiation properties and resolution control for the view factor calculations were set in ANSYS FLUENT via internal boundary

conditions on solid cells adjacent to fluid cells. The rest of the specified boundary conditions to perform the wind analysis are summarized below:

- ambient temperature of 300 K (80°F)
- no solar insolation (nonconservative assumption but irrelevant to the temperature differential)
- velocity inlet specified on the side of the wind
- pressure outlet specified on the opposing side of the wind
- wind velocity varied in the range of 0 to 6.706 m/s (0 to 15 mph)
- wind direction assumed parallel and orthogonal to the air vents
- adiabatic boundary assumed on the cask's bottom surface
- symmetry used when applicable
- surface emissivities set to 0.587 for stainless-steel surfaces inside the storage canister and 0.85 for carbon-steel surfaces outside the canister and for concrete surfaces

Figures 4-2 through 4-9 show the external boundary conditions. Each color in these figures refers to the type of applied boundary. Blue represents a velocity inlet, red represents a pressure boundary, yellow represents symmetry, black represents a wall, and green shows the cask vents used as interior cells, per ANSYS FLUENT nomenclature.

The ANSYS FLUENT porous media model requires the input of spent fuel effective thermal conductivity and flow resistance factors. Tables A-1 through A-3 of Appendix A and Table B-1 of Appendix B provide the values used for spent fuel effective thermal conductivity and flow resistance factors for the 3-D thermal models. Table 4-3 shows the total decay heat used in the analysis for the different casks considered in the evaluation.

4.7.3 Analyzed Axisymmetric Cases

The analyzed cases included low Reynolds k - ϵ to model the air flow turbulence between the liner and the MPC wall. For the helium flow inside the MPC, the calculated Reynolds and Rayleigh numbers are too low to consider a turbulent flow regime. Instead, a laminar regime was considered. DO was used to model the radiation transfer equation between the walls. Also, the effect of helium pressure inside the MPC was investigated. The control volume used the dry storage cask boundaries. In this control volume, the inlet and outlet ducts use either pressure or velocity boundaries, depending on the investigated case. In addition, a total decay heat load of 34 kW was assumed for all the axisymmetric cases. Table 4-2 shows the axisymmetric cases considered in the evaluation.

4.7.4 Applied Boundary Conditions for the Axisymmetric Model

A 2-D axisymmetric thermal model was used to analyze the thermal response of the HI-STORM 100 dry storage cask, as shown in Figures 4-10 and 4-11. A 2-D polar coordinate system is used to represent the dry storage cask system where only radial and axial directions are considered. The MPC section consists of two discrete regions—the basket region and the

peripheral region. The inner basket region represents the spent fuel storage basket, and the outer peripheral region represents the MPC downcomer. As shown in Figure 4-11, the inner region consists of three distinct regions—the spent fuel region, the bottom plenum, and the top plenum.

Porous media were used to model the spent fuel region, as well as the top and bottom plenums located in the center of the MPC. Flow-resistance factors (i.e., frictional and inertial) and temperature-dependent equivalent thermal conductivity (i.e., includes radiation and conduction heat transfer) are used to characterize the flow and heat transfer in the porous media regions. A laminar regime is used to model the flow of helium in this inner zone with a uniform porosity specified in ANSYS FLUENT. In the downcomer region (outer zone of the MPC model), a laminar regime is also considered. Helium at a pressure of about 7.2 bars is modeled as flowing from top to bottom in the downcomer region and from bottom to top in the spent fuel region.

For the air flow in the annular gap between the MPC and the overpack, the transitional low Reynolds k - ϵ turbulence model is used. Both the turbulent kinetic energy and its dissipation are used to model the average length and time scales of turbulence. Temperature-dependent equivalent thermal conductivity in the radial and axial directions, specific heat, density, porosity, and hydraulic losses are used to characterize the porous media. The calculated input values for the equivalent thermal conductivities in the radial and axial directions included the effect of both radiation and conduction heat transfer.

The ANSYS FLUENT CFD code was used to predict the spent fuel basket planar (radial) effective thermal conductivity (NUREG-2152, 2013). The effective axial thermal conductivity is estimated by area averaging the thermal conductivity of each material in a spent fuel basket cross-section. As a result, radiation heat transfer was not accounted for in the ANSYS FLUENT analysis, and zero values for the wall emissivities inside the canister were specified in the boundary conditions panel. DO was used to model radiation between walls in the axisymmetric model. A heat source was added to the cells representing the active spent fuel region. The local volumetric heat source term in each segment was determined by multiplying the basket active spent fuel length average source term with an axial power peaking factor. The four vents in the bottom and top of the cask, respectively, were represented by one continuous inlet at the bottom and one continuous outlet at the top. The model used the exact height for the inlet and outlet vents as in the physical model. As a result, the air vents flow area in the computational model was larger than the actual flow area specified in the physical model. As a remedy, porous media were used to introduce flow resistance along the channels to correct for the mass flow rate and the balance of momentum.

The HI-STORM 100 axisymmetric thermal model requires several simplifications. The most important step requires that the planar section of the MPC be homogenized. With each spent fuel storage cell replaced with an equivalent solid square, the MPC cross-section consists of a metallic grid (i.e., basket cell walls with each square cell space containing a solid storage cell square of temperature-dependent effective thermal conductivity) circumscribed by a circular ring (MPC shell). The four distinct materials in this section are homogenized spent fuel storage cell squares, stainless-steel structural material in the MPC (including neutron absorber sheathing), neutron absorber, and helium gas. Each of the four constituent materials in this section has a different conductivity.

In the axisymmetric model, the required simplification is performed by replacing the thermally heterogeneous spent fuel basket section by an equivalent conduction-only region using a 2-D CFD analysis (NUREG-2152, 2013). Because the rate of transport of heat in the spent fuel basket is influenced by radiation, which is a temperature-dependent effect, the equivalent conductivity of the spent fuel basket region must also be computed as a function of temperature. Also, it is recognized that the MPC section consists of two discrete regions; namely, the basket region and the peripheral region. The peripheral region is the space between the peripheral storage cells and the MPC shell. This is a helium-filled space surrounded by stainless-steel plates. Accordingly, as shown in Figure 4-10 for the vertical storage cask, the MPC cross-section is replaced by two homogenized regions with temperature-dependent conductivities. Temperature-dependent spent fuel effective thermal conductivity has been used to characterize the equivalent area that represents the spent fuel basket.

The two principal components of a loaded spent fuel basket are sandwich panels and SNF. These components have unequal conduction properties in the planar and axial directions. The spent fuel basket thermal modeling properly recognizes these differences by characterizing the effective conductivities in the two (planar and axial) directions. For computing the planar spent fuel basket conductivity, either a finite element-based model, such as the ANSYS code, or a finite volume-based CFD code, such as ANSYS FLUENT, can be employed. The principal inputs to the models are the spent fuel planar conductivities and the sandwich panel conductivities. The spent fuel basket axial conductivity is computed by an area-weighted sum of the cladding, helium, neutron absorber, and steel (box wall and sheathing) conductivities. In this evaluation, spent fuel pellet axial conduction and axial dissipation of heat by radiation are neglected in the calculation of the effective thermal conductivity in the axial direction.

Finally, the cask is simulated as being radially symmetric, having annular vents at the bottom and top with a buoyancy-induced flow in the annular space surrounding the heat-generating MPC cylinder. The annular gap between the MPC and the overpack is modeled explicitly, and the cask vents are represented by porous media, which specified effective inlet and outlet duct flow-resistance factors that are calculated separately.

Internal circulation of helium in the sealed MPC is modeled as flow in a porous media in the spent fuel basket region containing the SNF (including top and bottom plenum). The basket-to-MPC shell clearance is modeled as a helium-filled radial gap to include the downcomer flow in the thermal model. The downcomer region, as illustrated in Figure 4-10(a), consists of an azimuthally varying gap formed by the square-celled basket outline and the cylindrical MPC shell. In the FLUENT axisymmetric model, a single effective gap is used to model the downcomer region, as shown in Figures 4-10(b) and 4-11.

A low Reynolds $k-\epsilon$ model was used to represent turbulence in the air flow region (the annular gap formed by the MPC shell and overpack). Guidelines on the proper use of the low Reynolds $k-\epsilon$ turbulence model require the use of a finer mesh near the enclosing walls. As shown in Figure 4-12, a mesh was generated for this region such that the dimensionless distance y^+ , for the cells close to the wall, is close to unity for the axisymmetric model, thus fulfilling the requirements for the proper use of the low Reynolds $k-\epsilon$ turbulence model. The integration is performed all the way to the wall using an adequate fine generated mesh (as shown in Figure 4-12).

As mentioned earlier, the 2-D axisymmetric ANSYS FLUENT porous media model requires the input of effective thermal conductivity and flow-resistance factors. The effective thermal conductivity values used in the axisymmetric cases are shown in Table A-4 of Appendix A, and the flow-resistance factors are shown in Table B-1 of Appendix B.

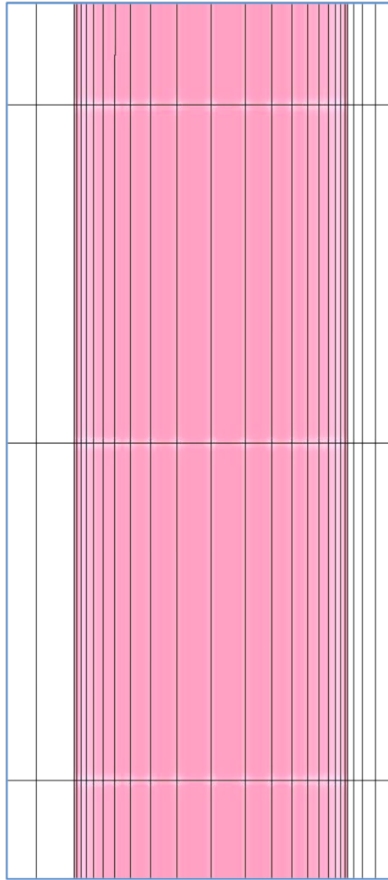


Figure 4-12 Mesh generated for the air annular gap of the axisymmetric model

Cases to Model the Effect of Humidity

As shown in Table 2-1, the effect of humidity was examined at ambient temperatures of 300 and 323 K, assuming a relative humidity of 0 percent, 50 percent, 70 percent, and 90 percent (for each temperature). For the calculations of the effect of humidity on air, ANSYS FLUENT requires the input of mass fractions of water vapor and air at the inlet boundary (inlet vent). These parameters are calculated as follows and provided to ANSYS FLUENT for each case.

For moist air, the total pressure is expressed as:

$$P_T = P_a + P_v \tag{1}$$

Where

P_T is the total pressure.

P_v is the partial pressure of water vapor.

P_a is the partial pressure of air.

The humidity ratio (sometimes called the specific humidity) is defined as:

$$W = \frac{m_v}{m_a} \quad (2)$$

Where m_v and m_a are the water vapor mass and air mass, respectively.

Also, relative humidity (Φ) is defined as the mole fraction of the water vapor (X_v) in a mixture to the mole fraction of the water vapor in a saturated mixture (X_s) at the same temperature and pressure:

$$\Phi = \frac{X_v}{X_s} \quad (3)$$

Using Dalton's law (Reid, "The Properties of Gases and Liquids," 1977) for a mixture of perfect gases, the mole fraction is equal to the ratio of the partial pressure to the total pressure.

$$X_v = \frac{P_v}{P_T} \quad (4)$$

Using Equations (3) and (4), one gets

$$\Phi = \frac{\frac{P_v}{P_T}}{\frac{P_s}{P_T}} = \frac{P_v}{P_s} \quad (5)$$

And from Equation (5)

$$P_v = \Phi P_s \quad (6)$$

From the ideal gas law:

$$m_v = \frac{P_v V M_v}{RT} \quad (7)$$

$$m_a = \frac{P_a V M_a}{RT} \quad (8)$$

Where

V is the total volume of the mixture.

M_v and M_a are the molecular weights of water and air, respectively.

\bar{R} is the universal gas constant.

T is the temperature.

Knowing that $M_v=18$ g/gmol and $M_a = 28.97$ g/gmol, using Equations (2), (7), and (8), one gets

$$W = \frac{m_v}{m_a} = \frac{P_v M_v}{P_a M_a} = 0.6219 \frac{P_v}{P_a} = 0.6219 \frac{P_v}{P_T - P_v} \quad (9)$$

For the axisymmetric thermal model, ANSYS FLUENT's boundary condition at the inlet vent used a pressure inlet with the following mass fractions of water vapor (mf_v) and air (mf_a):

$$mf_v = \frac{m_v}{m_a + m_v} = \frac{\frac{m_v}{m_a}}{\frac{m_a}{m_a} + \frac{m_v}{m_a}} = \frac{W}{W + 1} \quad (10)$$

$$mf_a = 1 - mf_v = \frac{1}{W + 1} \quad (11)$$

As such, the inlet water vapor and air mass fraction were specified in ANSYS FLUENT, as shown in Table 4-5 at the two different assumed ambient temperatures of 300 and 323 K. As can be seen from Table 4-5, water vapor increases as air humidity is increased from 0 to 90 percent.

Table 4-5 Mass Fraction Specified at Inlet Vent for Humidity Analyses

Ambient Temperature K (°F)	Φ (%)	P_s (Pa)	P_v (Pa)	W kg of water vapor/kg of air	mf_v (%)	mf_a (%)
300 (80)	0	3,567	0	0	0	1
-	50	3,567	1,784	0.011	0.011	0.989
-	70	3,567	2,497	0.016	0.015	0.985
-	90	3,567	3,210	0.020	0.020	0.98
323 (120)	0	12,350	0	0	0	1
-	50	12,350	6,175	0.040	0.039	0.961
-	70	12,350	8,645	0.058	0.055	0.945
-	90	12,350	11,115	0.077	0.071	0.929

As shown in Table 2-1, the effect of ambient temperature was examined assuming ambient temperatures of 300 K (80°F), 305 K (90°F), 311 K (100°F), 316 K (110°F), and 322 K (120°F) using a steady-state analysis. This study used a transient analysis to investigate the transient thermal response of a dry storage cask to a sudden change in the ambient temperature. In the transient analysis, the ambient temperature was suddenly changed from 300 K (80°F) to 322 K (120°F). The transient analysis examined the time it took the dry storage cask to reach a new steady state.

The investigation of the effect of the heat load assumed total decay heats of 22, 24, 26, 28, 30, 32, and 34 kW. The pressure inlet and pressure outlet were specified at the inlet and outlet vents of the axisymmetric ANSYS FLUENT thermal model and steady-state analyses were performed to determine the effect of the total decay heat on the predicted PCT.

The investigation of the effect of the dry storage cask elevation (i.e., ambient pressure) assumed the dry storage cask was located at elevations of 0, 500, 1,000, and 1,500 m above sea level. Steady-state analyses used in this investigation specify the pressure inlet and pressure outlet at the inlet and outlet vent, respectively. The analysis examined the effect of the air density at the inlet vents (as it varies with ambient pressure) on the predicted PCT.

As mentioned earlier, the effect of the worst-case wind scenario was also studied using the axisymmetric model. The 3-D analyses determined that the worst-case scenario was for an aboveground vertical cask with two vents (postulated case). In this case, the wind is assumed to be blowing at 4.4703 m/s (10 mph), with wind direction parallel to the air vents. Using the 3-D worst-case scenario, an equivalent axisymmetric steady-state case was found by comparing the PCT. Then, a transient case scenario was performed using the inlet mass flow rate (determined by comparing the 3-D and 2-D cases, which resulted in the same PCT) and the pressure outlet for the inlet and outlet vents, respectively. The transient analysis examined the time it took the dry storage cask to reach a new steady state.

4.8 Discussion of Results

An analysis of the results from the 3-D thermal models described in previous sections for the different cask configurations determined the effect of wind magnitude and direction on the cask's thermal performance. Specifically, it determined the effect of low-speed wind (wind in the range of 0 to 6.706 m/s (0 to 15 mph) and wind direction (parallel and orthogonal to air vents) on

the predicted PCT. Tables 4-6 through 4-15 summarize the effect of wind magnitude and direction on the thermal performance of dry storage casks (predicted PCT) considered in this evaluation. Results from the axisymmetric model of the vertical aboveground cask described in previous sections were analyzed to determine the effect of ambient temperature, air humidity, elevation, wind, and total decay heat in the cask on the cask's thermal performance. Specifically, they determined the effect of these parameters on the predicted PCT. The following sections discuss the results from these analyses.

4.8.1 Wind Effect on the Underground Casks

Table 4-6 shows how the thermal performance of underground casks is affected by the magnitude of wind. The predicted PCT increases as wind speed increases until wind speed reaches about 2.235 m/s (5 mph). Table 4-6 also shows that PCT starts to decrease with a further increase in wind speed. This behavior is explained by examining how the air mass flow rate varies in the air-cooling channel. As the air mass flow rate increases, PCT decreases because of the improved cooling effect by convection. The air vents in the underground cask occupy the entire cask perimeter. The flow rate of the air mass moving through the cask is directly proportional to the pressure difference between the inlet and outlet vents. As wind speed increases from quiescent conditions to 2.235 m/s (5 mph), air blowing at the outlet vent acts as flow resistance by increasing the pressure at the exit. Examination of the air mass flow rate in Table 4-6 shows that the flow resistance at the exit reaches its maximum at a wind speed of 2.235 m/s (5 mph) (lowest air mass flow rate). As such, the air mass flow rate reaches its minimum and the PCT reaches its maximum at 2.235 m/s (5 mph). The pressure difference between the inlet and the outlet vents decreases between 0 and 2.235 (5 mph). Then, as wind speed increases beyond 2.235 m/s (5 mph), the pressure difference starts to increase. As a result, the mass flow increases (improving convective cooling) and the PCT decreases.

4.8.2 Wind Effect on the Vertical Aboveground Casks

Table 4-7 shows the effect of wind speed on the vertical dry storage cask with four inlet and four outlet vents (like the HI-STORM 100). Overall, the analysis shows that wind had a slight positive effect on the cask's thermal performance for average wind speed [wind speed of about 2.235–3.576 (5–8 mph)], as reported by NOAA (NOAA, www.noaa.gov). As the wind speed increases, the cooling air mass flow rate increases and the PCT decreases. It should be noted that the calculated temperatures for the base case (quiescent conditions) and windy conditions are only shown to illustrate the effect of wind on the cask's thermal performance. The predicted PCT may be higher than the NRC's recommended limit for normal storage, but it is only because the analysis was intentionally set up this way to produce conservative results. This may also apply to the results presented for other casks in this study. Also, the objective of these analyses was to determine the relative increase, as compared to the base cases.

For the case of a postulated two-vent vertical dry storage cask design, when wind direction is normal to the air vents, the thermal performance was positively affected as wind speed increased. As the wind speed increased, the mass flow rate through the air vents increased and the PCT decreased, as shown in Table 4-8. When wind direction is parallel to the air vents, the magnitude of the wind adversely affects the thermal performance of the cask. The parallel wind at the inlet and exit vents acts as flow blockage. When wind is parallel to the inlet vents, as the wind speed increases, less air flows into the inlet vents (since wind acts as a flow blockage). Similarly, when wind is parallel to the outlet vents, as the wind speed increases, the

air acts as a flow blockage and less air flows through the outlet vents. As such, when wind direction is parallel to the vents, air flow through the duct is decreased and the PCT is increased, as shown in Table 4-9. It should be mentioned that this analysis corresponds to an extreme case, because the NRC has not certified a cask design with only two air vents. The case was included in the study to determine how wind affects the thermal performance of this design. The wind analysis results from a two-vent vertical cask show that this design is very sensitive to low-speed wind and that parallel wind has a strong negative effect on the cask's thermal performance.

The effect of wind on the thermal performance of the cask was noticeably high in the case of the two-vent cask design with a 4.4703-m/s (10-mph) wind parallel to the cask vents. The analysis of the 4.4703-m/s (10-mph) wind case used a steady-state approach. To further investigate this scenario, a transient analysis of the case was undertaken using an axisymmetric representation of the cask. First, an equivalent axisymmetric model was built to reproduce the same PCT as the 3-D base-case model and the worst-case scenario [4.4703-m/s (10-mph) wind], as shown in Table 4-9. The transient analysis first assigned the initial condition of the equivalent base case and then applied a sudden change reflecting the conditions from the worst-case scenario at the cask boundaries (air vents). As shown in Tables 4-17 and 4-18, 95 percent of the PCT change between the base case and the worst-case scenario was reached after 256.5 hours (about 10.68 days).

4.8.3 Wind Effect on the Horizontal Aboveground Casks

The wind study for horizontal aboveground casks used standardized and advanced NUHOMS casks. For the standardized cask, the analyses results showed that the magnitude and direction of wind did not have any significant effect on the thermal performance of the cask, as shown in Tables 4-10 and 4-11. Neither the magnitude nor the direction of the wind is expected to affect the thermal performance of the cask because of the placement of the vents. As described in Section 4.3.1, the vents in the standardized NUHOMS casks are located on the sides of the cask and are not in direct contact with either parallel or normal wind. The normal wind (wind blowing perpendicular to the air vents) will not be a factor on the thermal performance because of the presence of either another cask on the side or a wall at the end of a row of casks located in an ISFSI.

For the advanced aboveground horizontal NUHOMS casks, the inlet vent is located on the front of the cask and the outlet vent is located on the roof, as described in Section 4.3.1. For the case of wind parallel to the vents, the thermal performance of the dry storage cask was not significantly affected, as shown in Table 4-14. When the wind is blowing towards the front of the cask (wind direction perpendicular to the inlet vent), more air is admitted to the cask and the thermal performance of the cask is improved, as shown in Table 4-12.

Since the advanced cask design locates the air outlet vent on top of the cask, the study also included the case for wind blowing perpendicular to the back of the cask to determine how this affects the cask's thermal performance. Table 4-13 shows the steady-state analysis results with wind directed to the back of the cask for wind speed varying in the range of 0 to 6.706 m/s (0 to 15 mph). As the wind speed increased, less air flowed through the cask and the PCT increased. The predicted PCT reached its maximum at a wind speed of 4.4703 m/s (10 mph) and then declined as the air flow rate through the cooling channel started to increase. To further investigate this case, a transient analysis was performed. The case used steady base

case results as the initial conditions, as shown in Table 4-13. Then, using the worst-case scenario, the environmental conditions suddenly changed, with wind blowing towards the back of the storage cask at 10 mph, as shown in Table 4-13. Tables 4-15 and 4-16 show a 95 percent PCT change between the base case and the worst-case scenario after 10 days. The transient analysis results indicate that steady-state conditions will be reached after 10 days of windy conditions with wind speed remaining constant for 10 days.

4.8.4 Aboveground Vertical Cask Axisymmetric Model

The study used an axisymmetric model to investigate the effect of the ambient temperature, using steady-state simulations. Table 4-19 shows the effect of the ambient temperature on the predicted PCT in the dry storage cask. The PCT increases by 8 K (14.4°F) for every 5.6 K (10°F) increase in the ambient temperature.

In the transient analysis, used to study the effect of ambient temperature, the initial condition set the ambient temperature at 300 K (80°F). Then the ambient temperature was suddenly changed to 322 K (120°F). As shown in Tables 4-20 and 4-21, 95 percent of the PCT change between 300 and 322 K (80 and 120°F) was reached after 7 days.

The effect of elevation was investigated using a steady-state analysis based on the axisymmetric model. The analyses varied the elevation from 0 to 1500 m (0 to 4921.5 ft). As the elevation is increased, the air density decreases due to the decrease in the ambient pressure. As a result, the mass flow rate decreased and the PCT increased. As shown in Table 4-22, the PCT increases by about 6 K (11°F) for every 500 m (1640.5 ft) of increased elevation.

To study the effect of heat load, steady-state analyses, based on the axisymmetric model, varied heat loads in the range of 20 to 34 kW. As the decay heat increased, the PCT also increased. As shown in Table 4-23, the PCT increases by about 22 K (40°F) for every 2 kW increase in heat load.

The effect of ambient air humidity was investigated using a steady-state analysis based on the axisymmetric model. The analyses were performed at ambient temperatures of 300 K (80°F) and 323 K (120°F) with a relative humidity of 0, 50 percent, 70 percent, and 90 percent. As the humidity increases, the ambient air contains more water vapor. As water vapor has larger thermal conductivity and heat capacity than dry air, more heat is absorbed from the cask by humid air. As such, the PCT will decrease as the relative humidity is increased for both ambient temperatures considered in this study. At an ambient temperature of 300 K (80°F), the PCT decreased by 0.6 K (1°F) for every 20 percent increase in the relative humidity (in the 50 to 90 percent range). At an ambient temperature of 323 K (120°F), the PCT decreased by 2.2 K (4°F) for every 20-percent increase in relative humidity (in the 50 to 90 percent range). The rate of decrease in the predicted PCT is higher for the ambient temperature 323 K (120°F) case than for the ambient temperature 300 K (80°F) case because of the higher moisture content change for every 20 percent change in relative humidity in the latter, as shown in Tables 4-24 and 4-25.

Table 4-6 Effect of Wind Speed on Predicted PCT for HI-STORM 100U Cask

Wind Speed m/s (mph)	Air Mass Flow Rate (kg/s)	Peak Cladding Temperature (K)
0 (0)	0.227	646
1.3411 (3)	0.189	675
2.235 (5)	0.152	693
3.1292 (7)	0.168	684
4.4703 (10)	0.192	677
6.706 (15)	0.218	661

**Table 4-7 Effect of Wind Speed on Predicted PCT for HI-STORM 100 Cask
with Four Vents**

Wind Speed m/s (mph)	Mass Flow Rate (kg/s)	Peak Cladding Temperature (K)
Base Case	0.156	712
0.8941 (2)	0.146	713
2.235 (5)	0.166	710
3.1292 (7)	0.204	703
4.4703 (10)	0.267	690
6.706 (15)	0.409	669

**Table 4-8 Effect of Wind Speed on Predicted PCT for HI-STORM 100 Cask with
Two Vents (Wind Perpendicular to Air Vents)**

Wind Speed m/s (mph)	Mass Flow Rate (kg/s)	PCT (K)
Base case	0.0958	744.6
2.235 (5)	0.1003	737.4
4.4703 (10)	0.1389	733.8
6.706 (15)	0.2320	714.5

**Table 4-9 Effect of Wind Speed on Predicted PCT for HI-STORM 100 Cask with
Two Vents (Wind Parallel to Air Vents)**

Wind Speed (mph)	Mass Flow Rate (kg/s)	PCT (K)
Base case	0.0958	744.6
2.235 (5)	0.0531	787.2
4.4703 (10)	0.0165	886.5
6.706 (15)	0.0388	879

Table 4-10 Effect of Wind Speed on Predicted PCT for Standardized NUHOMS Cask (Frontal Wind Direction)

Wind Speed m/s (mph)	Mass Flow Rate (kg/s)	PCT (K)
Base Case	0.2512	680.4
2.235 (5)	0.2486	679.6
4.4703 (10)	0.2522	680.4
6.706 (15)	0.2539	679.9

Table 4-11 Effect of Wind Speed on Predicted PCT for Standardized NUHOMS Cask (Side Wind Direction)

Wind Speed m/s (mph)	Mass Flow Rate (kg/s)	PCT (K)
Base Case	0.2512	680.4
2.235 (5)	0.2536	679.9
4.4703 (10)	0.2536	679.6
6.706 (15)	0.2518	679.8

Table 4-12 Effect of Wind Speed on Predicted PCT for Advanced NUHOMS Cask (Frontal Wind Direction)

Wind Speed m/s (mph)	Mass Flow Rate (kg/s)	PCT (K)
Base Case	0.3495	675
2.235 (5)	0.7875	666
4.4703 (10)	1.509	661
6.706 (15)	2.2569	657

Table 4-13 Effect of Wind Speed on Predicted PCT for Advanced NUHOMS Cask (Back Wind Direction)

Wind Speed m/s (mph)	Mass Flow Rate (kg/s)	PCT (K)
Base Case	0.3495	675
2.235 (5)	0.2789	680.6
4.4703 (10)	0.23	689.9
6.706 (15)	0.26	683

Table 4-14 Effect of Wind Speed on Predicted PCT for Advanced NUHOMS Cask (Side Wind Direction)

Wind Speed m/s (mph)	Mass Flow Rate (kg/s)	PCT (K)
Base Case	0.3495	675
2.235 (5)	0.3009	677
4.4703 (10)	0.2902	677
6.706 (15)	0.2959	677

Table 4-15 Transient PCT for Advanced NUHOMS Cask During Worst-Case Scenario (Back Wind Direction)

Time (Days)	Mass Flow Rate (kg/s)	PCT (K)
0	0.3495	675.0
1	0.19	677.8
2	0.20	680.6
3	0.20	682.9
4	0.21	684.8
5	0.21	686.2
6	0.21	687.3
7	0.22	688.2
8	0.22	688.6
9	0.22	688.8
10	0.22	689.1
11	0.22	689.4
12	0.23	689.5

Table 4-16 Advanced NUHOMS Worst-Case Transient Scenario

Case	Mode of Analysis	Wind Conditions	PCT (K)	Time to Reach 95 % of PCT
Advanced TN Back Wind Base Case	Steady	No Wind	675	N/A
Advanced TN Back Wind Worst-Case Scenario	Steady	4.4703 m/s (10 mph) Wind	689.9	N/A
Two Vents Worst-Case Scenario	Transient	4.4703 m/s (10 mph) Wind	$675 + 0.95(689.9 - 675) = 689.1$	10 days

Table 4.17 Aboveground Vertical Cask with Two Vents—Transient Scenario

Time (Days)	PCT (K)
0	744.6
1	779.5
2	810.4
3	829.2
4	842.7
5	852.9
6	860.7
7	866.7
8	871.4
9	875
10	877.9
11	880
12	881.7
13	883.1
14	884.1
15	884.9
16	885.5
17	885.9
18	886.2
19	886.4
20	886.6
21	886.7

Table 4-18 Aboveground Vertical Cask with Two Vents—Worst-Case Transient Scenario

Case	Mode of Analysis	Wind Conditions	PCT (K)	Time to Reach 95% of PCT
Two Vents Base Case	Steady	No Wind	744.6	N/A
Two Vents Worst-Case Scenario	Steady	4.4703 m/s (10 mph) Wind	886.5	N/A
Two Vents Worst-Case Scenario	Transient	4.4703 m/s (10 mph) Wind	$744.6 + 0.95(886.5 - 744.6) = 879.4$	256.4 hrs (10.68 days)

Table 4-19 Effect of Ambient Temperature on Predicted PCT (Steady-State Analysis)

Ambient Temperature K (°F)	Air Inlet Density (kg/m ³)	PCT (K)
300 (80)	1.1766	712
305 (90)	1.1559	720
311 (100)	1.1353	728
316 (110)	1.1153	736
322 (120)	1.0961	744

Table 4-20 Transient PCT for the Effect of Ambient Temperature

Time (Days)	PCT (K)
0	712
1	721.5
2	729.8
3	734.9
4	738.1
5	740.2
6	741.6
7	742.4
8	743
9	743.3

Table 4-21 Effect of Ambient Temperature on Predicted PCT (Transient Analysis)

Case	Mode of Analysis	Ambient Temperature K (°F)	PCT (K)	Time to Reach 95% of PCT
Base Case	Steady	300 (80)	712	N/A
Worst-Case Scenario	Steady	322 (120)	744	N/A
Worst-Case Scenario	Transient	Step change 300 (80) → 322 (120)	$712 + 0.95(744 - 712) = 742.4$	167.83hrs (~7 days)

Table 4-22 Effect of Elevation on Predicted PCT (Steady-State Analysis)

Elevation (m)	Inlet Air Density (kg/m ³)	PCT (K)
0	1.1766	712
500	1.11	718
1,000	1.0434	724
1,500	0.9767	731

Table 4-23 Effect of Total Decay Heat on Predicted PCT (Steady-State Analysis)

Q (kW)	PCT (K)
20	556
22	578
24	600
26	623
28	645
30	668
32	690
34	712

Table 4-24 Effect of Humidity on Predicted PCT at Ambient Temperature of 300 K (Steady-State Analysis)

Ambient Temperature K (°F)	Density (kg/m ³)	Φ (%)	PCT (K)
300 (80)	1.177	0	712.6
	mixture	50	710.9
	mixture	70	710.3
	mixture	90	709.7

Table 4-25 Effect of Humidity on Predicted PCT at Ambient Temperature of 323 K (Steady-State Analysis)

Ambient Temperature K (°F)	Density (kg/m ³)	Φ (%)	PCT (K)
323 (120)	1.0928	0	745
	Mixture	50	739
	Mixture	70	737
	Mixture	90	734.7

5.0 CONCLUSIONS

This report describes the application of the ANSYS FLUENT commercial computational fluid dynamics (CFD) code to examine the effect of environmental conditions on the thermal performance of dry storage casks. The research included the effect of wind speed and direction, elevation, total decay heat, air humidity, and ambient temperature. The magnitude of the environmental variables was selected using available data from National Oceanic and Atmospheric Administration (NOAA) and *ASHRAE Handbook Fundamentals* (ASHRAE, 1997). Thermal analyses used thermal models of underground casks, aboveground vertical casks, and aboveground horizontal casks. These analyses included the use of 3-D models as well as axisymmetric representation of a vertical-ventilated cask. Based on the analysis results, the report reached the following conclusions:

- Wind magnitude mainly affects the underground cask design included in this study. As wind speed increases, predicted peak cladding temperature (PCT) increases for a range of wind speeds of 0 to 2.235 meters per second (m/s) [0 to 5 miles per hour (mph)], as compared to quiescent conditions. At a wind speed of about 2.235 m/s (5 mph), the PCT reached the maximum predicted value. At higher wind speeds, the PCT starts to decrease. Therefore, low wind speed should be considered in the thermal evaluation as a normal environmental variable. This specific analysis examined the effect on this type of underground design and determined that a wind speed of 2.235 m/s (5 mph) will result in the maximum predicted cladding temperature. A thermal evaluation should be performed for other underground designs to determine how wind affects the cask's thermal performance, as part of the thermal evaluation for normal storage conditions.
- Wind slightly enhanced the thermal performance of an aboveground vertical cask with at least four air vents. The predicted PCT decreases as wind speed increases.
- Wind enhanced the thermal performance of a postulated two-vent cask design when the wind blows in the direction normal (perpendicular) to the air vents. The predicted PCT decreases as wind speed increases.
- Wind negatively affected the thermal performance of a postulated two-vent vertical cask design when wind blew parallel to the air vents. At a wind speed of 4.4703 m/s (10 mph), the PCT reaches its maximum predicted value and then starts to decrease at higher values.
- For the postulated two-vent vertical aboveground cask, about 95 percent of PCT change was reached in 10 days for the case where wind direction is parallel to the air vents (worst-case scenario).
- Wind does not significantly affect the performance of the aboveground horizontal standardized NUHOMS casks. The vents in the standardized NUHOMS overpack are located on the sides of the overpack and therefore are not in direct contact with either parallel or normal wind.
- Wind does not significantly affect the advanced NUHOMS casks when the wind direction is blowing parallel to the air vents.

- Wind enhances the thermal performance of the advanced NUHOMS cask when wind blows in the direction normal (perpendicular) to the cask front. The predicted PCT decreases as wind speed increases.
- Wind affects the thermal performance of the advanced NUHOMS casks when the wind direction is normal (perpendicular) to the back of the cask. The PCT reaches its maximum predicted value at a wind speed of 4.4702 m/s (10 mph) and then starts to decrease.
- Based on a transient analysis, about 95 percent of PCT change is reached in 10 days when the wind direction is normal (perpendicular) to the back of the advanced NUHOMS cask with a magnitude of 10 mph. For this design, the applicant should include the effect of back wind when there is no sufficient margin.
- Ambient temperature inversely affects the thermal performance of a spent fuel dry storage cask. The PCT increases by 8 Kelvin (K) [14.4 degrees (°) Fahrenheit (F)] for every 5.6 K (10°F) increase in ambient temperature.
- Based on a transient analysis, about 95 percent of the PCT change between the 300 and 322 K (80 and 120°F) steady-state cases is reached after 7 days. Measured temperatures suggest that, to bound all sites, the SAR thermal evaluation should consider seasonal variations.
- Elevation inversely affects the thermal performance of a spent fuel dry storage cask. The PCT increased by 6 K (11°F) for every 500 m increase in elevation.
- Ambient air humidity enhances the thermal performance of a spent fuel dry storage cask. At an ambient temperature of 300 K (80°F), the PCT decreased by 0.6 K (1°F) for every 20 percent relative humidity increase in the range of 50 to 90 percent. At an ambient temperature of 323 K (122°F), the PCT decreased by 2.2 K for every 20 percent relative humidity increase in the range of 50 to 90 percent.
- As the total decay heat is increased, the PCT is negatively affected. The PCT increases by 22 K (40°F) for every 2 kW increase in the total heat load of the cask.

6.0 REFERENCES

ASHRAE Handbook Fundamentals, Atlanta, GA, 1997.

American Society of Mechanical Engineers (ASME), "Standard for Verification and Validation in Computational Fluid Dynamics and Heat Transfer," V&V 20-2009.

Fluent User Guide Version 6, Fluent Inc., New Hampshire, 2006.

Holtec International, HI-STORM 100 Final Safety Analysis Report, December 2005.

Holtec International, HI-STORM 100 Final Safety Analysis Report, December 2007.

Idelchik, I.E., "Handbook of Hydraulic Resistance," 3rd edition, CRC Press, 1993.

JANAF Thermochemical Tables, Third Edition, published by the American Chemical Society and the American Institute of Physics for the National Bureau of Standards, Volume 14, 1985.

NOAA, National Oceanic and Atmospheric Administration, Web page: www.noaa.gov.

NUREG-1536, "Standard Review Plan for Spent Fuel Dry Storage Systems at a General License Facility," Washington, DC, July 2010.

Reid, Robert C, John M. Prausnitz, and Thomas K. Sherwood, *The Properties of Gases and Liquids*, McGraw-Hill Book Company, Inc, 3rd edition, 1977.

Sparrow, E. M. and A. L. Loeffler, Jr., "Longitudinal laminar flow between cylinders arranged in regular array," *A.I.Ch.E. Journal*, Volume 5, No. 3, pp. 3253–30, 1959.

TRW Environmental Safety Systems, Inc., "Spent Nuclear Fuel Effective Thermal Conductivity Report," Prepared for U.S. Department of Energy, July 11, 1996.

Transnuclear, Inc., Standardized NUHOMS Final Safety Analysis Report, January 2006.

Transnuclear, Inc., Standardized Advanced NUHOMS Final Safety Analysis Report, August 2008.

NUREG-2152, "Computational Fluid Dynamics Best Practice Guidelines for Dry Cask Applications," Washington, DC, March 2013.

Title 10, "Energy," of the *Code of Federal Regulations*, Part 71, "Packaging and Transportation of Radioactive Material."

Title 10, "Energy," of the *Code of Federal Regulations*, Part 72, "Licensing Requirements for the Independent Storage of Spent Nuclear Fuel, High-Level Radioactive Waste, and Reactor-Related Greater Than Class C (GTCC) Waste."

APPENDIX A

EFFECTIVE THERMAL CONDUCTIVITY

The tightly packed spent fuel rods within the stainless-steel spent fuel canisters are modeled as a homogeneous solid material region with a specified uniform heat generation rate and an effective thermal conductivity. The anisotropic thermal conductivity option in the ANSYS FLUENT code was used to represent the different effective conductivities of the spent fuel region in the axial and radial directions. The effective conductivity in the axial direction was represented as an area-weighted fraction of the conductivity of Zircaloy-4, using an area-weighted ratio of the cladding to the total cross-section of the homogeneous region. This relationship was implemented in ANSYS FLUENT, based on the temperature-dependent thermal conductivity of Zircaloy-4. The effective thermal conductivity (k_{eff}) values in the radial direction of the spent fuel region were obtained as a function of temperature using the standard k_{eff} methodology (TRW report, 1996). The k_{eff} values used in the canister are based on a calculational “database” generated by a separate two-dimensional (2-D) ANSYS FLUENT analysis for unconsolidated spent fuel using a detailed 2-D model (NUREG-2152, 2013).

The radial and axial k_{eff} values calculated for a helium environment inside the canister are shown in Tables A-1 through A-4 for the different configurations used in this report. This is the approach generally employed in a typical spent fuel dry storage cask safety analysis report (SAR) to determine peak cladding temperatures in spent fuel dry storage casks when the spent fuel assemblies are modeled as a homogeneous material (i.e., porous media). Following the documented form of the basic k_{eff} model, this approach produced an effective thermal conductivity for the homogeneous spent fuel region as a function of the local temperature on the computational domain. The model is implemented in ANSYS FLUENT as temperature-dependent k_{eff} values.

Table A-1 Spent Fuel Radial and Axial K_{eff} for the 3-D Model of the Aboveground Vertical Cask

Temperature (K)	K radial (W/(m-K))	K axial (W/(m-K))
366	2.0738	7.39
505	2.5507	8.01
644	3.0976	8.54
783	3.5783	9.089

Table A-2 Spent Fuel Radial and Axial K_{eff} for 3-D Model of the Underground Vertical Cask

Temperature (K)	K radial (W/(m-K))	K axial (W/(m-K))
366	0.445	1.35
505	0.703	1.268
644	1.045	1.431

Table A-3 Spent Fuel Radial and Axial K_{eff} for the 3-D Model of the Horizontal Cask

Temperature (K)	K radial (W/(m-K))	K axial (W/(m-K))
366	1.3	1.27
505	2.3	2.04
644	3.3	2.278

Table A-4 Spent Fuel Axial and Radial K_{eff} for the Axisymmetric Model

Temperature (K)	K radial (W/(m-K))	K axial (W/(m-K))
366	2.0738	7.39
505	2.5507	8.01
644	3.0976	8.54

APPENDIX B

FLOW RESISTANCE

To obtain the porous media flow-resistance parameters (frictional and inertial losses), three-dimensional (3-D) computational fluid dynamics calculations are performed (NUREG-2152, 2013). The analyzed control volume consists of the assembly walls surrounding the spent fuel rods and associated grid spacers. All flow areas and passages are modeled explicitly. The case should reflect and model flow losses in the expected operating conditions (pressure and average gas temperature) when spent fuel is inside the dry storage cask. The present analysis used a total pressure of 7 atmospheres (atm) and a temperature of 505 K.

The ANSYS FLUENT code (FLUENT, 2006) defined the porous media flow-resistance model as:

$$\frac{\Delta P}{L} = D\mu V + C\left(\frac{1}{2}\rho V^2\right) \quad (1)$$

Where

ΔP is the porous media pressure drop.

V is the superficial fluid velocity.

L is the length of porous media.

μ is the fluid viscosity.

ρ is the fluid density.

D is the viscous resistance parameter.

C is the inertial resistance parameter.

In dry cask applications, the C factor is not as dominant as the D factor because of the low fluid velocity that exists inside the canister. As such, the entire pressure drop was assumed to be entirely caused by frictional losses. As a verification, the inertial coefficient (C) can be computed from correlations using area contractions and expansion (Idelchik, 1993) in the assembly to show that the second term in Equation (1) is negligible. Additionally, it would be conservative to neglect C , because predicted peak cladding temperatures will be slightly higher.

By definition, the frictional pressure drop is:

$$\frac{\Delta P}{L} = \frac{f}{D_h} \frac{1}{2} \rho V^2 \quad (2)$$

Where D_h is the hydraulic diameter.

Knowing that:

$$\text{Re} = \frac{\rho V D_h}{\mu}$$

We get:

$$\frac{\Delta P}{L} = \frac{f \text{ Re}}{2} \frac{\mu}{D_h^2} V$$

Usually the friction factor in the laminar regime as shown in a Moody diagram will have the following form:

$$f = \frac{A}{\text{Re}} \quad (3)$$

As an illustration, the frictional coefficient due to the pressure drop for laminar flow in a pipe has been experimentally determined to correspond to the following expression:

$$f = \frac{64}{\text{Re}}$$

Thus:

$$\frac{\Delta P}{L} = \frac{32\mu}{D_h^2} V$$

For an array of solid rods, as is the case of a nuclear spent fuel assembly from a boiling-water or a pressurized-water reactor, the value of the factor “A” can be determined from available literature (Sparrow, 1959). The “A” factor has been found to have a value around 100, depending on the pitch-to-diameter ratio and the porosity of the array.

Using Equation (1) and neglecting the inertial term because of the low fluid velocities existing inside the storage canister, the dominant contributor to pressure drop is the viscous effect. The pressure drop through the rod array can be simplified to:

$$\frac{\Delta P}{L} = D\mu V \quad (4)$$

Then

$$D = \frac{A}{2D_h^2} \quad (5)$$

For laminar flow inside a pipe, $A = 64$, and the input frictional resistance in ANSYS FLUENT should be:

$$D = \frac{32}{D_h^2}$$

Also, by definition:

$$f = \frac{4\tau_w}{\frac{1}{2}\rho V^2} \quad (6)$$

Where τ_w is the wall shear stress.

The porous media frictional flow-resistance values for D were calculated using both pressure drop and shear stress. Both methods should lead to similar results. Using the shear stress ANSYS FLUENT output data, the viscous resistance parameter D is obtained using the combination of Equations (2), (4), and (6). The following expression is obtained:

$$D = \frac{4\tau_w}{\mu V D_h} \quad (7)$$

If the pressure loss data were used, the expression for D is obtained from Equation (4) as follows;

$$D = \frac{\Delta P}{L\mu V} \quad (8)$$

From the CFD calculations of the spent fuel assembly, the wall shear stresses or pressure drop values should be obtained separately for bare fuel rods and fuel rods plus grid straps. Depending on the approach used to calculate the friction factors, Equation (7) or (8) is used to obtain the parameter D. Table B-1 provides the calculated frictional porous media flow resistance parameters.

Table B-1 Frictional Porous Media Flow Resistance Factors Used in ANSYS FLUENT

Region	HI-STORM 100U 3-D Model (1/m ²)	HI-STORM 100 Model (1/m ²)	HI-STORM 100 Axisymmetric Model (1/m ²)
Active region	7.41E5	1.7E6	1.7E6
Bottom inactive region	8.82E5	1.7E6	1.7E6
Top inactive region	4.4E5	1.7E6	1.7E6

NRC FORM 335 (12-2010) NRCMD 3.7	U.S. NUCLEAR REGULATORY COMMISSION BIBLIOGRAPHIC DATA SHEET <i>(See Instructions on the reverse)</i>	1. REPORT NUMBER (Assigned by NRC, Add Vol., Supp., Rev., and Addendum Numbers, if any.) NUREG-2174 Draft			
2. TITLE AND SUBTITLE Impact of Variation in Environmental Conditions on the Thermal Performance of Dry Storage Casks	3. DATE REPORT PUBLISHED				
	<table border="1"> <tr> <td data-bbox="1143 344 1321 373">MONTH</td> <td data-bbox="1326 344 1497 373">YEAR</td> </tr> <tr> <td data-bbox="1143 380 1321 415">February</td> <td data-bbox="1326 380 1497 415">2015</td> </tr> </table>	MONTH	YEAR	February	2015
MONTH	YEAR				
February	2015				
5. AUTHOR(S) Jorge Solis and Ghani Zigh	4. FIN OR GRANT NUMBER 				
	6. TYPE OF REPORT Technical				
8. PERFORMING ORGANIZATION - NAME AND ADDRESS (If NRC, provide Division, Office or Region, U. S. Nuclear Regulatory Commission, and mailing address; if contractor, provide name and mailing address.) Division of Spent Fuel Management Office of Nuclear Material Safety and Safeguards U.S. Nuclear Regulatory Commission Washington, D.C. 20555-0001					
9. SPONSORING ORGANIZATION - NAME AND ADDRESS (If NRC, type "Same as above", if contractor, provide NRC Division, Office or Region, U. S. Nuclear Regulatory Commission, and mailing address.) Same as above.					
10. SUPPLEMENTARY NOTES					
11. ABSTRACT (200 words or less) <p>This report evaluates spent fuel dry storage cask thermal impact of varying environmental conditions and transient thermal behavior when subjected to a sudden boundary condition change. The results showed that, for the underground cask design, the peak cladding temperature (PCT) increases for low-speed wind and starts to decrease at higher speed. For vertical aboveground casks with four vents, PCT decreased as wind speed increased. For a postulated two-air-vent vertical dry storage cask, when wind direction is normal to the air vents, PCT decreased as the wind speed increased. When wind direction is parallel to the air vents of the two-air-vent cask, PCT increased as the wind speed increased. For horizontal aboveground casks with air vents located on the side, the wind speed and direction did not have any significant impact. For horizontal aboveground casks with inlet vents located on the front, when wind direction is facing the front of the cask, the thermal performance of the cask was improved, but when wind direction was parallel to the cask front, no significant effect was observed. These results can be used as additional guidance when considering the thermal impact of the environmental factors in the thermal performance of dry storage systems.</p>					
12. KEY WORDS/DESCRIPTORS (List words or phrases that will assist researchers in locating the report.) Spent Fuel Environmental Variables Wind Speed CFD Best Practice Guidelines Standard Review Plan SRP CFD	13. AVAILABILITY STATEMENT unlimited				
	14. SECURITY CLASSIFICATION <i>(This Page)</i> unclassified				
	<i>(This Report)</i> unclassified				
	15. NUMBER OF PAGES				
16. PRICE					



Federal Recycling Program



**UNITED STATES
NUCLEAR REGULATORY COMMISSION**
WASHINGTON, DC 20555-0001

OFFICIAL BUSINESS



**NUREG-2174
Draft**

**Impact of Variation in Environmental Conditions on the Thermal
Performance of Dry Storage Casks**

February 2015